



Published in final edited form as:

Cell. 2021 September 16; 184(19): 4904–4918.e11. doi:10.1016/j.cell.2021.07.037.

## Parallel pathways for recruiting effector proteins determine centromere drive and suppression

Tomohiro Kumon<sup>1</sup>, Jun Ma<sup>1</sup>, R. Brian Akins<sup>1</sup>, Derek Stefanik<sup>1</sup>, C. Erik Nordgren<sup>1</sup>, Junhyong Kim<sup>1</sup>, Mia T. Levine<sup>1</sup>, Michael A. Lampson<sup>1,2,\*</sup>

<sup>1</sup>Department of Biology, School of Arts and Sciences, University of Pennsylvania, Philadelphia, PA 19104, USA

<sup>2</sup>Lead Contact

### Summary

Selfish centromere DNA sequences bias their transmission to the egg in female meiosis. Evolutionary theory suggests that centromere proteins evolve to suppress costs of this “centromere drive”. In hybrid mouse models with genetically different maternal and paternal centromeres, selfish centromere DNA exploits a kinetochore pathway to recruit microtubule-destabilizing proteins that act as drive effectors. We show that such functional differences are suppressed by a parallel pathway for effector recruitment by heterochromatin, which is similar between centromeres in this system. Disrupting the kinetochore pathway with a divergent allele of CENP-C reduces functional differences between centromeres, whereas disrupting heterochromatin by CENP-B deletion amplifies the differences. Molecular evolution analyses using *Murinae* genomes identify adaptive evolution in proteins in both pathways. We propose that centromere proteins have recurrently evolved to minimize the kinetochore pathway, which is exploited by selfish DNA, relative to the heterochromatin pathway that equalizes centromeres, while maintaining essential functions.

### Graphical Abstract

\*Correspondence: lampson@sas.upenn.edu.

#### Author Contributions

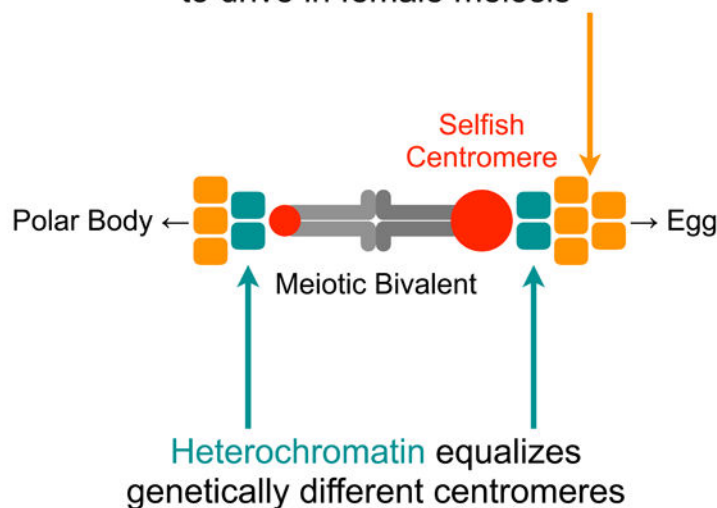
Conceptualization, T.K., M.T.L. and M.A.L.; Methodology, T.K.; Software, T.K., D.S. and C.E.N.; Investigation, T.K., J.M. and R.B.A.; Writing – Original Draft, T.K.; Writing – Review & Editing, T.K., M.T.L. and M.A.L.; Funding Acquisition, T.K., J.K., M.L.T. and M.A.L.; Resources, J.K. and M.A.L.; Supervision, M.A.L.

**Publisher's Disclaimer:** This is a PDF file of an unedited manuscript that has been accepted for publication. As a service to our customers we are providing this early version of the manuscript. The manuscript will undergo copyediting, typesetting, and review of the resulting proof before it is published in its final form. Please note that during the production process errors may be discovered which could affect the content, and all legal disclaimers that apply to the journal pertain.

#### Declaration of Interests

The authors declare no competing interests.

Selfish centromeres recruit more kinetochore proteins to drive in female meiosis



### In brief

Recurrent evolution of centromere proteins minimizes functional differences between genetically different centromeres by balancing the pathways that promote and suppress drive by selfish sequences.

### Keywords

Meiotic Drive; Selfish Genetic Elements; Evolutionary Arms Race; Centromere; Kinetochore; Heterochromatin

### Introduction

Centromere evolution is paradoxical in that both repetitive centromere DNA and centromere-binding proteins evolve rapidly despite the conserved requirement of centromeres for faithful chromosome segregation (Henikoff et al., 2001; Lampson and Black, 2017; Malik and Henikoff, 2001; Melters et al., 2013; Schueler et al., 2010). Centromere DNA repeat monomer sequence and repeat copy number diverge between even closely related species. Repeat copy number also varies within species, for example, between human individuals or between mouse strains (Iwata-Otsubo et al., 2017; Langley et al., 2019). To explain this rapid evolution, the centromere drive hypothesis proposes that selfish centromere DNA sequences (either monomer sequence variants or repeat number expansions) drive in female meiosis by increasing their transmission rate to the egg. Potential deleterious consequences of driving centromeres, such as meiotic segregation errors, would select for centromere-binding protein variants that suppress these fitness costs (Finseth et al., 2021; Fishman and Saunders, 2008; Henikoff et al., 2001). New selfish DNA variants subsequently arise to start another cycle of drive and suppression in a continual evolutionary arms race.

Our previous work leveraged natural variation in mouse centromere DNA to study the molecular mechanisms of centromere drive (Akera et al., 2017, 2019; Chmátal et al., 2014; Iwata-Otsubo et al., 2017). Selfish centromeres in these model systems recruit more effector proteins that preferentially destabilize interactions with tyrosinated microtubules on the cortical side of an asymmetric meiosis I spindle, allowing them to detach from microtubules that would otherwise direct them to the polar body. Microtubule detachment and reattachment reorients the selfish centromeres toward the egg side of the spindle (Akera et al., 2017, 2019) (Figure 1A). This reorientation depends on BUB1 kinase at kinetochores, which phosphorylates pericentromeric histone H2A. Phosphorylated H2A recruits Shugoshin-2 (SGO2), which recruits microtubule destabilizing proteins such as MCAK and the chromosome passenger complex (CPC) (Akera et al., 2019) (Figure 1B, kinetochore pathway). In one intra-species *Mus musculus domesticus* hybrid, selfish centromeres with expanded minor satellite DNA repeats assemble more centromere chromatin containing the histone H3 variant CENP-A (Iwata-Otsubo et al., 2017). These expanded centromeres also form larger kinetochores with more BUB1 kinase, leading to more effectors (inner centromere proteins such as SGO2, CPC, and MCAK) (Akera et al., 2019). In this hybrid, the larger centromeres are from a standard laboratory strain (either CF-1 or C57BL/6J), which is crossed to a wild-derived strain (CHPO) with smaller centromeres. Thus, the centromeres of paired homologous chromosomes within a meiotic bivalent are both genetically and functionally different in the hybrid (Figure 1C). These findings show how selfish centromeres can drive by recruiting more effectors. How centromere-binding proteins can evolve to suppress the costs of drive remains an open question despite being a crucial component of the centromere drive model. Details of the fitness costs are unclear, but they likely depend on functional differences between paired centromeres in meiosis and would therefore be suppressed by reducing these differences.

## Results

### **The parallel pathway model for drive and suppression provides three testable predictions.**

Based on our finding that selfish centromeres drive by recruiting more effectors, we propose that functional differences between centromeres can be suppressed by equalizing effector recruitment via a second pathway. This equalization would render genetically different centromeres functionally equivalent. This model incorporates previous findings that in addition to the kinetochore pathway, which acts through BUB1 kinase, effectors are also recruited through a heterochromatin pathway. Pericentromeric heterochromatin recruits the CPC, which recruits SGO2 and MCAK (Figure 1B, heterochromatin pathway) (Abe et al., 2016; Ainsztein et al., 1998; Higgins and Prendergast, 2016; Kang et al., 2011; Marston 2015). In our CHPO hybrid model system (Figure 1C), the kinetochore pathway is asymmetric: we observe higher levels of the kinetochore proteins HEC1/NDC80 and CENP-C on larger vs smaller centromeres (Chmátal et al., 2014; Iwata-Otsubo et al., 2017). In contrast, the heterochromatin pathway is symmetric: the heterochromatin mark, H3K9me3, is equal on the two sides of each bivalent (Figure 1D and 1E) (Iwata-Otsubo et al., 2017). These observations suggest that, in this system, selfish centromere DNA exploits the kinetochore pathway to make genetically different centromeres also functionally different, with larger centromeres recruiting more effectors. In contrast, the heterochromatin

pathway appears insensitive to selfish DNA, recruiting effectors equally. We propose that centromere protein evolution suppresses functional differences by minimizing the contribution of the asymmetric kinetochore pathway to effector recruitment, relative to the symmetric heterochromatin pathway.

Evolution of the kinetochore pathway is constrained by its indispensable role in mitotic and meiotic chromosome segregation. Nevertheless, proteins may evolve to weaken the pathway by reducing interactions between centromere-binding proteins and DNA or between proteins leading to effector recruitment (Figure 1F). Similarly, evolution of heterochromatin proteins is constrained by numerous vital heterochromatin-dependent cellular functions (Allshire and Madhani, 2017). Inner centromere proteins (such as the CPC) that interact with heterochromatin may evolve, however, to increase effector recruitment. Finally, overall effector levels are also constrained because microtubule destabilizing activity is necessary to correct kinetochore-microtubule attachment errors, but excessive destabilizing activity weakens attachments necessary for anaphase segregation and activates the spindle assembly checkpoint (Godek et al., 2014). According to our parallel pathway model, a new centromere DNA variant can exploit the kinetochore pathway to recruit more effectors by strengthening interactions with any centromere-binding protein that contacts the DNA: CENP-A, the CENP-A chromatin assembly machinery, or other proteins that link centromere chromatin to the kinetochore (e.g., CENP-C or CENP-T). To suppress functional differences between centromeres, the centromere protein network recurrently evolves to minimize the kinetochore pathway relative to the heterochromatin pathway while maintaining essential functions.

Here we test three predictions from the parallel pathway model. First, when the asymmetric kinetochore pathway is weakened, we predict that centromeres become functionally more similar due to the symmetric heterochromatin pathway. We selected CENP-C as a key scaffold protein in the kinetochore pathway that is known to evolve rapidly under positive selection (Klare et al., 2015; Schueler et al., 2010; Talbert et al., 2004). Under the parallel pathway model, CENP-C interfaces have co-evolved with interacting partners to modulate effector recruitment. Thus, introducing a divergent allele of CENP-C in mouse cells (e.g., rat CENP-C, in which 32% of the amino acid sequence is different) is predicted to disrupt such interactions and weaken the kinetochore pathway (Figure 1G). Second, when the symmetric heterochromatin pathway is weakened, we predict that the asymmetric kinetochore pathway makes a relatively larger contribution to effector recruitment. Genetically different centromeres in our hybrid model system should therefore become functionally more different. To target pericentromeric heterochromatin, we deleted CENP-B, which is the only centromeric chromatin component that is dispensable for core centromere function. CENP-B is recently acquired in mammals and fission yeast from a pogo-like transposase (Casola et al., 2007; Kipling and Warburton, 1997), and several domesticated transposases regulate heterochromatin (Gao et al., 2020; Jangam et al., 2017; Nozawa et al., 2010; Yang et al., 2017). In mouse and human cultured cells and fission yeast, CENP-B contributes to pericentromeric heterochromatin formation via heterochromatin protein recruitment (Nakagawa et al., 2002; Okada et al., 2007; Otake et al., 2020), so deleting CENP-B should weaken the heterochromatin pathway (Figure 1H). Mammalian CENP-B can also contribute to the kinetochore pathway via CENP-C recruitment (Fachinetti

et al., 2015), so the functional consequences of CENP-B deletion in our model need to be tested. Third, if proteins in the kinetochore and heterochromatin pathways have evolved to modulate effector recruitment, we predict signatures of positive selection in multiple protein domains involved in effector recruitment. In contrast, the previous model of an arms race limited to interactions between centromere DNA and DNA-binding proteins only predicts rapid evolution of protein domains involved in DNA binding (Henikoff et al., 2001; Malik and Henikoff, 2001). Our observations are consistent with all three predictions, supporting our parallel pathway model for drive and suppression.

### **Introducing a divergent CENP-C allele weakens the kinetochore pathway and makes centromeres functionally more symmetric.**

To weaken the kinetochore pathway, we targeted CENP-C because it serves as a hub for recruiting kinetochore proteins. Our model predicts that CENP-C has co-evolved with interacting partners to modulate effector recruitment, so that an allele from another species will disrupt these interactions and weaken the kinetochore pathway (Figure 1G, Prediction 1). To test this prediction, we selected divergent alleles from rat and from the African striped mouse *Rhabdomys pumilio* as model organisms close to mouse with divergent centromere DNA and proteins (Figure 2A) (Cazaux et al., 2013; Gibbs et al., 2004; Mallarino et al., 2018; Takeiri et al., 2013). Because protein interfaces change by genetic drift as well as by selection, alleles from closely related species minimize incompatibilities coming from stochastic changes. We introduced GFP-tagged divergent alleles (or the mouse allele as a control) into mouse oocytes in the presence of endogenous CENP-C (Supplementary Figure 1A–1B). We find that rat CENP-C expression reduces effector recruitment, as represented by SGO2 staining, compared to mouse CENP-C expression (Figure 2B). This result is consistent with our model prediction and could reflect differences between mouse and rat CENP-C in their recruitment to centromeres or in their interactions with other kinetochore proteins. For example, evolution at an interface with CENP-A nucleosomes or with CENP-B may disrupt rat CENP-C recruitment to centromeres. Alternatively, CENP-C evolution might impact the domains that mediate interactions with other kinetochore proteins involved in SGO2 recruitment. We find that mouse and rat CENP-C are equally recruited and incorporated into mouse centromeres (Figure 2C and Supplementary Figure 1C–1E), indicating functional changes at an interface with other kinetochore proteins.

In contrast to our results with rat CENP-C, *R. pumilio* CENP-C is recruited at higher levels to mouse centromeres compared to mouse CENP-C (Figure 2D), with similar expression levels as measured by cytoplasmic GFP (Supplementary Figure 1F). Consistent with this result, effector recruitment is also increased in cells expressing *R. pumilio* CENP-C (Figure 2E). Together, these findings show that different CENP-C interfaces, with centromere chromatin or with other kinetochore proteins, have changed through rodent evolution to modulate effector recruitment (Figure 2F). Furthermore, differences between *R. pumilio* and mouse CENP-C localization to mouse centromeres suggest that mouse CENP-C has evolved to weaken its interactions with centromere chromatin.

Rat CENP-C expression provides an experimental tool to specifically weaken the kinetochore pathway, without affecting heterochromatin (Figure 2G, Supplementary Figure

1G), allowing us to test our prediction that genetically different centromeres become functionally more similar in our hybrid model system (Figure 1G, Prediction 2). As a functional readout of centromere asymmetry, we analyzed chromosome position on the spindle at metaphase I (Figure 2H, Supplementary Figure 2A–2B). Chromosome position is sensitive to differences in interactions with spindle microtubules between centromeres of homologous chromosomes, which are paired in a meiotic bivalent. If the paired centromeres are genetically and functionally similar, then chromosomes align at the spindle equator in a typical metaphase configuration. In our CHPO hybrid model systems, paired centromeres are genetically and functionally different, and bivalents are positioned off-center on the spindle, with the larger centromere closer to its attached pole (Akerá et al., 2019; Chmátal et al., 2014). Manipulations that make these genetically different centromeres functionally more similar will lead to positioning closer to the spindle equator, as previously shown by manipulating BUB1 kinase to equalize MCAK levels on larger and smaller centromeres (Akerá et al., 2019). Conversely, manipulations that make the centromeres functionally more different will position bivalents closer to the poles. We find that expression of rat CENP-C in CHPO hybrid oocytes (Figure 1C) leads to bivalents positioned closer to the spindle equator (Figure 2I), without affecting meiotic progression (Supplementary Figure 2C). This result indicates that the paired larger and smaller centromeres are functionally more similar, consistent with the prediction that the symmetric heterochromatin pathway becomes relatively more dominant when the asymmetric kinetochore pathway is weakened (Figure 1G, Prediction 2). We also tested *R. pumilio* CENP-C expression but did not find changes in chromosome position (Supplementary Figure 1H), suggesting that the modest increase in effector recruitment (Figure 2E) does not impact microtubule destabilizing activity enough to be detected in our assay.

### **Deleting CENP-B weakens the heterochromatin pathway and makes centromeres functionally more asymmetric.**

To determine the contribution of CENP-B to effector recruitment, we created *Cenpb* null mice using CRISPR genome editing (Supplementary Figure 3A–3C). We find that loss of CENP-B weakens both the kinetochore and heterochromatin pathways, as shown by reduced CENP-C and H3K9me3 staining, respectively (Figure 3A). These results are consistent with previous findings that CENP-B contributes to CENP-C recruitment and to formation of pericentromeric heterochromatin (Fachinetti et al., 2015; Okada et al., 2007; Otake et al., 2020). We also find reduced effector recruitment, as represented by SGO2 staining (Figure 3A), consistent with the idea that CENP-B recruits effectors through the kinetochore and heterochromatin pathways.

The known functions of CENP-B suggest two hypotheses for how it might affect centromeres in our CHPO hybrid model system. First, as the only centromere protein known to recognize a specific DNA sequence (the CENP-B box in repetitive centromere DNA) (Masumoto et al., 1989), CENP-B could be exploited by selfish larger centromeres with more CENP-B boxes to increase asymmetry via the kinetochore pathway. Second, CENP-B may suppress functional differences between centromeres by increasing the symmetric heterochromatin pathway. To test these hypotheses, we generated *Cenpb* null mice with paired larger and smaller centromeres through two generations of crosses (Figure

3B), and analyzed kinetochore pathway asymmetry and functional differences between centromeres. Due to technical limitations (Supplementary Figure 3D), we were unable to measure transmission bias in these animals. To determine the impact of CENP-B on the kinetochore pathway, we analyzed CENP-C in meiotic bivalents with paired larger and smaller centromeres in second-generation hybrid *Cenpb*<sup>-/-</sup> oocytes. CENP-C was reduced to a similar extent on both larger and smaller centromeres (Supplementary Figure 3E) and consistent with this equivalent reduction, the kinetochore asymmetry remained intact (Figure 3C). Therefore, CENP-B does not contribute to asymmetry in the kinetochore pathway, arguing against the first hypothesis that selfish centromere DNA exploits the kinetochore pathway via CENP-B.

To test the second hypothesis, that CENP-B acts as a suppressor through the symmetric heterochromatin pathway (Figure 1H), we examined functional differences between centromeres in second-generation hybrid oocytes, using the chromosome position assay (Figure 2H). We find that asymmetric bivalents with genetically different centromeres are positioned more off-center, closer to the spindle poles, in *Cenpb*<sup>-/-</sup> compared to control *Cenpb*<sup>+/-</sup> oocytes (Figure 3D). In contrast, we find no effect on positioning of symmetric bivalents with genetically identical centromeres in the same cells, and meiotic progression is similar in control and *Cenpb*<sup>-/-</sup> oocytes (Supplementary Figure 2D). Together these findings indicate that positioning of asymmetric bivalents closer to spindle poles in *Cenpb*<sup>-/-</sup> oocytes is due to increased functional differences between paired centromeres. This result is opposite to the result for rat CENP-C expression, which specifically weakens the kinetochore pathway (Figure 2B and 2G) and reduces functional asymmetry (Figure 2I). Therefore, although CENP-B deletion also weakens the kinetochore pathway, the dominant effect is to weaken a different pathway that equalizes centromeres, leading to increased functional asymmetry. Several lines of evidence indicate that this equalization pathway acts through heterochromatin: CENP-B is an established regulator of heterochromatin (Nakagawa et al., 2002; Okada et al., 2007; Otake et al., 2020), heterochromatin is similar on larger and smaller centromeres in our hybrid (Figure 1D) and reduced in *Cenpb*<sup>-/-</sup> oocytes (Figure 3A), and heterochromatin is an established pathway to recruit effector proteins (Abe et al., 2016; Ainsztein et al., 1998; Higgins and Prendergast, 2016; Kang et al., 2011; Marston 2015). We conclude that CENP-B suppresses functional differences between centromeres through the heterochromatin pathway. It is also possible, however, that CENP-B equalizes centromeres through an uncharacterized pathway independent of kinetochore assembly and heterochromatin.

### **Proteins in the kinetochore and heterochromatin pathways have signatures of recurrent adaptive evolution.**

The original model of centromere drive and suppression posits an arms race between selfish centromere DNA and DNA-binding proteins such as CENP-A (Henikoff et al., 2001; Malik and Henikoff, 2001). This model predicts adaptive evolution of centromere protein domains that physically interact with DNA, and conservation of domains and other centromere proteins that do not bind DNA. In contrast, our parallel pathway model predicts signatures of recurrent adaptive evolution in protein domains leading to effector recruitment, including those that do not directly contact centromere DNA (Figure 4A). These changes could

Author Manuscript

Author Manuscript

Author Manuscript

either weaken the kinetochore pathway or strengthen the heterochromatin pathway to make genetically different centromeres functionally more similar (Figure 1F). Rapid evolution of centromere proteins has been reported in several eukaryotic lineages, but there are no mechanistic studies of drive in these lineages (Finseth et al., 2015; Malik and Henikoff, 2001; Schueler et al., 2010; van der Lee et al., 2017). To analyze centromere protein evolution in a system where we have identified drive effectors, we tested for signatures of positive selection in Murinae. Because the sparseness of the phylogenetic tree of currently available Murinae genomes limits our statistical power to detect positive selection, we sequenced six additional genomes (Figure 4B) using linked-read whole genome sequencing (10x Genomics). Each genome was assembled onto the *Mus musculus* reference genome (mm10) with LongRanger and *de novo* assembled with Supernova (see STAR Methods and Supplementary Table 1). Sampling evolutionary time more comprehensively increases our opportunities to observe adaptive changes (and minimize false positives from stochastic changes by genetic drift), especially those adaptive changes that are common to multiple independent lineages. Thus, these genomes provide a valuable resource for molecular evolution approaches in mouse as a mammalian model organism, such as our analyses of centromere proteins discussed below.

Author Manuscript

Author Manuscript

Low rates of nonsynonymous substitutions, which change the encoded amino acid, relative to synonymous substitutions (dN/dS) indicate purifying selection, as deleterious substitutions are selected against. Higher dN/dS indicates either adaptive evolution or loss of constraint, necessitating further analysis to identify signatures of positive selection (Echave et al., 2016; Sironi et al., 2015). We calculated dN/dS for all annotated mouse-rat orthologous genes. We find that multiple genes encoding centromere proteins have high dN/dS relative to the genome overall (Figure 4C), and the average dN/dS for these genes is significantly higher than for any other subcellular compartment (Figure 4D). We selected 46 genes with well-characterized centromere functions to analyze for signatures of positive selection based on phylogenetic analysis, using PAML (Yang, 2007). Consistent with our prediction, we find such signatures at multiple genes in the kinetochore and heterochromatin pathways (Figure 4E).

Author Manuscript

Author Manuscript

Extensive previous studies of centromere organization and function have established functional modules which can recruit drive effectors either directly or indirectly (Figure 4A). To fit our observations into this framework, we assigned genes to these modules (Supplementary Figure 4). One module is CENP-A chromatin. Selfish centromere DNA can increase effector recruitment by expanding CENP-A chromatin through increased deposition of CENP-A nucleosomes. This process depends on a specialized histone chaperone, HJURP, which is targeted to centromeres by the MIS18 complex through interactions with CENP-C or CENP-I (Dunleavy et al., 2009; Foltz et al., 2009; Fujita et al., 2007; Moree et al., 2011; Shono et al., 2015). We find rapid evolution of HJURP, MIS18BP1, CENP-I, and the domain of CENP-C that interacts with the MIS18 complex (Figure 4E and 5A). In contrast, heterochromatin proteins such as HP1 paralogs and SUV39H1, which are not specific to centromeres/pericentromeres, are highly conserved (Supplementary Table 2), consistent with the idea that heterochromatin broadly suppresses selfish genetic elements regardless of the underlying DNA sequence (Allshire and Madhani, 2017). These findings suggest that selection acts on the CENP-A chromatin assembly pathway to prevent expansion, but



selfish centromere DNA does not exploit the heterochromatin pathway, consistent with our observation that genetically different centromeres have symmetric heterochromatin in our intra-species and inter-species hybrids (Figure 1D and our unpublished data).

Under our model (Figure 1B), selfish centromere DNA can also recruit more effectors through the kinetochore pathway by strengthening direct interactions with CENP-A or with the constitutive centromere-associated network (CCAN), leading to larger kinetochores and more BUB1 kinase. Proteins can subsequently adapt by weakening interactions either with DNA or with other kinetochore proteins (Figure 4A, DNA interface and kinetochore assembly). Within the CCAN, CENP-C and CENP-T connect CENP-A chromatin to kinetochore proteins. The middle part of CENP-C interacts with CENP-A nucleosomes, while the N-terminus interacts with the MIS12 kinetochore complex (Petrovic et al., 2016; Weir et al., 2016). Similarly, the CENP-TWSX nucleosome-like complex contacts centromere DNA, and the other end of CENP-T interact with MIS12 and NDC80 kinetochore complexes (Cortes-Silva et al., 2020; Nishino et al., 2012; Veld et al., 2016). Consistent with our model, we detect signatures of positive selection in the chromatin-interacting domains and the kinetochore-interacting domains of both CENP-C and CENP-T (Figure 5A and 5B). In contrast, the DNA-interacting domain of CENP-B is conserved, consistent with our finding that selfish centromere DNA does not exploit CENP-B. Unlike in other eukaryotic lineages such as monkeyflower, fly, and primates (Finseth et al., 2015; Malik and Henikoff, 2001; Schueler et al., 2010), we do not detect signatures of positive selection in the part of CENP-A that can be aligned in Murinae species, but the N-terminal tail is duplicated in some species and therefore difficult to analyze by standard methods (Supplementary Figure 5A). Diversification of the CENP-A N-terminal tail is also observed in plants, where crosses between strains expressing different alleles exhibit zygotic segregation errors and genome elimination (Maheshwari et al., 2015).

In the kinetochore module, proteins can adapt to weaken the kinetochore pathway by reducing either kinetochore assembly or BUB1 binding to the kinetochore (Figure 4A). We find rapid evolution of the kinetochore proteins DSN1, KNL1, and NDC80. DSN1 is a component of the MIS12 complex, which assembles onto the CCAN and serves as a platform for binding KNL1 and the NDC80 complex (Petrovic et al., 2014). KNL1 contains multiple protein docking motifs, including repeated MELT motifs that recruit BUB1 kinase (Musacchio and Desai, 2017). Thus, changes in DSN1 and KNL1 can regulate kinetochore assembly and BUB1 recruitment. Consistent with the possibility that these interfaces evolve to modulate effector recruitment, we find signatures of positive selection in the MELT motifs of KNL1 (Figure 5C). NDC80 is the major microtubule binding protein in the kinetochore, but we find signatures of positive selection in the coiled-coil domain and not in the microtubule interacting domain. The coiled-coil domain recruits the SKA complex, which stabilizes kinetochore-microtubule attachment (Veld et al., 2019) and could be involved in counteracting destabilizing activities exploited by selfish centromeres.

Although selfish centromere DNA is likely unable to exploit heterochromatin to drive, inner centromere proteins can adapt to increase effector recruitment through the heterochromatin pathway relative to the kinetochore pathway in our model. In the inner centromere module (Figure 4A), INCENP is a scaffold component of the CPC that interacts directly with

heterochromatin and indirectly with SGO1/2 (Abe et al., 2016; Ainsztein et al., 1998; Kang et al., 2011; Tsukahara et al., 2010). Other CPC components, Borealin and Survivin, regulate SGO1/2 recruitment and pericentromeric localization (Kelly et al., 2010; Tsukahara et al., 2010; Wang et al., 2010; Yamagishi et al., 2010). The catalytic component of the CPC is Aurora B kinase, which phosphorylates kinetochore substrates to destabilize microtubule interactions and is thus a potential drive effector. We find that positive selection shapes the domains of INCENP that interact with Borealin/Survivin, with HP1, and with Aurora B (Figure 5D), suggesting that INCENP can adapt to selfish centromere DNA by modulating its localization to pericentromeric heterochromatin and ultimately the recruitment of SGO1/2 and Aurora B. Furthermore, we find rapid evolution of SGO2, suggesting that it can also tune the relative strength of the two pathways through mutations that modulate its recruitment by either pathway. In comparison, SGO1 is a paralog of SGO2 that does not recruit MCAK (Yao and Dai, 2012) and does not have signatures of positive selection, suggesting that evolutionary pressure to regulate MCAK recruitment shapes SGO2 evolution. Overall, our molecular evolution analyses show signatures of positive selection in both the kinetochore and heterochromatin pathways. We find these changes both in domains that interact directly with DNA and in protein-protein interaction domains leading to recruitment of drive effectors. These results are consistent with our parallel pathway model for drive and suppression, but not with a simpler model of an arms race limited to centromere DNA and DNA binding proteins.

## Discussion

Here we propose a parallel pathway model for drive and suppression of selfish centromeres: centromere DNA can exploit the kinetochore pathway to increase effector recruitment, and centromere protein evolution can make centromeres functionally equivalent by minimizing the contribution of the kinetochore pathway relative to the heterochromatin pathway (Figure 6A). This model predicts that disruption of either pathway will reduce effector (e.g., SGO2) recruitment, but the functional consequences will depend on which pathway is affected. Centromeres become either functionally more similar if the asymmetric kinetochore pathway is weakened, or more different if the symmetric heterochromatin pathway is weakened. In our experiments, either introduction of a divergent allele of CENP-C or deletion of CENP-B leads to SGO2 reduction to a similar extent (Figure 2B and 3A). However, genetically different centromeres in CHPO hybrid oocytes become functionally more similar when rat CENP-C is expressed (Figure 2I), whereas they become functionally more different when CENP-B is deleted (Figure 3D). The CENP-C results are consistent with our model prediction that natural selection has acted on CENP-C interfaces involved in effector recruitment, so a divergent rat CENP-C interacts less well with mouse binding partners in the kinetochore pathway. Therefore, expression of rat CENP-C weakens the asymmetric kinetochore pathway, making the symmetric heterochromatin pathway relatively more dominant. In contrast, CENP-B deletion weakens the symmetric heterochromatin pathway, as shown by reduced H3K9me3, making the asymmetric kinetochore pathway more dominant. Loss of CENP-B also reduces CENP-C recruitment but does not affect the asymmetry between larger and smaller centromeres (Figure 3C).

Our molecular evolution analyses show adaptive evolution in multiple centromere proteins and in specific domains that interact with CENP-A chromatin or with other proteins leading to effector recruitment (Figure 4 and 5). The previous model of a molecular arms race limited to interactions between centromere DNA and DNA-interacting proteins (such as CENP-A) (Henikoff et al., 2001) does not explain the more widespread recurrent evolution of centromere proteins. An alternative explanation, independent of centromere drive, is that the selective pressure may be related to non-centromere functions. For example, kinetochore proteins are repurposed for neural development in fly and worm (Cheerambathur et al., 2019; Zhao et al., 2019), and KNL1 (also known as CASC5) is implicated in human brain size regulation (Javed et al., 2018; Shi et al., 2016). However, such non-centromere functions have not been identified more broadly in eukaryotes. In contrast, our parallel pathway model predicts recurrent evolution of proteins in both pathways to equalize centromeres by weakening the kinetochore pathway or strengthening the heterochromatin pathway. In our model, selfish centromere DNA evolves to exploit the kinetochore pathway by recruiting more of a protein that ultimately recruits effectors. To suppress functional differences between centromeres, proteins in the kinetochore pathway can adapt to minimize the impact of selfish centromere DNA on kinetochore formation or effector recruitment. Indeed, our findings with *R. pumilio* CENP-C indicate that mouse CENP-C is not optimized for maximum binding to mouse centromeres, effectively weakening the kinetochore pathway (Figure 2D). Furthermore, proteins in the heterochromatin pathway such as CENP-B can adapt to increase effector recruitment equally at all centromeres, or INCENP and SGO2 can adapt by modulating their recruitment by either pathway (Figure 6A). The acidic domain of CENP-B is implicated in recruiting heterochromatin proteins (Otake et al., 2020), and the number of negatively charged amino acids in this domain is recurrently changed in mammals (Supplementary Figure 5B and 5C). Although these changes are not analyzed in PAML, they suggest that CENP-B may have evolved to regulate pericentromeric heterochromatin. Overall, a protein network for effector recruitment can adapt to minimize asymmetric recruitment by selfish centromere DNA, while maintaining essential functions of the kinetochore and of microtubule destabilizing factors for accurate chromosome segregation.

Our results suggest an explanation for the conservation of CENP-B in mammals, as well as the presence of its binding sequence, the CENP-B box, at most mammalian centromeres with the notable exception of the Y chromosome. Although CENP-B is the only centromere protein known to bind a specific DNA sequence in mammals, neither the protein nor the binding sequence is essential for centromere function (Amor et al., 2004; Hudson et al., 1998; Kapoor et al., 1998; Logsdon et al., 2019; Perez-Castro et al., 1998). We propose that CENP-B is conserved because it suppresses functional differences between centromeres by strengthening the heterochromatin pathway (Figure 6B), consistent with a more general function of heterochromatin in suppressing many selfish genetic elements (Allshire and Madhani, 2017). This CENP-B function is important only when centromeres of homologous chromosomes are different, which would frequently occur in outbred populations. Loss of CENP-B therefore increases functional difference between larger and smaller centromeres in our hybrid model, but does not significantly impair fertility or viability in inbred laboratory strains (Hudson et al., 1998; Kapoor et al., 1998; Perez-Castro et al., 1998). A potential

cost of increasing heterochromatin, however, is that its invasion into CENP-A chromatin disrupts centromere function (Ohzeki et al., 2016). We therefore propose that mammalian CENP-B has acquired an additional function to maintain CENP-A chromatin, by recruiting CENP-C and CENP-A chromatin regulators (Fachinetti et al., 2015; Otake et al., 2020) (Figure 6B). Consistent with this idea, CENP-A chromatin is reduced in *Cenpb* null oocytes (Supplementary Figure 3F). By regulating both CENP-A chromatin and heterochromatin, alternative functions of CENP-B in different chromatin environments may suppress functional differences between centromeres through heterochromatin while maintaining centromere function. CENP-B can suppress differences between centromeres only if its functions are insensitive to expansion of the number of CENP-B binding sites; otherwise it would contribute to higher levels of effector recruitment by DNA repeat expansions. Indeed, we find that CENP-B does not contribute to asymmetry in CENP-C recruitment between larger and smaller centromeres (Figure 3C), despite 6- to 10-fold differences in minor satellite sequences containing CENP-B boxes (Iwata-Otsubo et al., 2017). This result suggests that CENP-B recruits CENP-C only within the CENP-A chromatin domain, so that CENP-B binding outside of this domain does not strengthen the kinetochore pathway. Furthermore, the heterochromatin symmetry between larger and smaller centromeres (Figure 1D) suggests that although CENP-B contributes to initiating heterochromatin formation, for example by recruiting an H3K9 methyltransferase, heterochromatin spreading does not depend on the number of CENP-B boxes. Initiation of heterochromatin propagation is a common mechanism to regulate heterochromatin formation, as in the example of X inactivation where XIST initiates heterochromatinization of the entire chromosome (Allshire and Madhani, 2017). Thus, CENP-B functions in CENP-A chromatin and heterochromatin are insensitive to repeat expansion. A centromere variant completely lacking CENP-B boxes, however, will lose to an existing centromere in female meiosis because it will recruit less effectors by both the kinetochore and heterochromatin pathways. Therefore, CENP-B boxes are maintained at most centromeres (Figure 6A), but this selective pressure does not affect the Y chromosome, which never experiences female meiosis and does not bind CENP-B (Gamba and Fachinetti, 2020).

Genetic conflict between selfish centromere DNA and centromere-binding proteins potentially explains the complexity of eukaryotic centromeres. Opportunities for selfish genetic elements to exploit the chromosome segregation machinery are not limited to female meiosis, as selfish plasmids (e.g., 2-micron plasmids in budding yeast) benefit by maximizing their transmission to daughter cells in mitosis (Malik and Henikoff, 2009; Rizvi et al., 2017). These opportunities are limited by the strong epigenetic component of most eukaryotic centromeres, which are not defined by specific DNA sequences. Centromeres cannot be completely independent of the underlying DNA sequence, however, because some protein must interact with DNA, so different sequences can have different binding affinities or impact the structure of the centromeric nucleosome complex (Allu et al., 2019). The presence of multiple pathways to form a kinetochore (e.g., via CENP-ACLN and CENP-TWSX connected by CENP-HIKM, or via CENP-OPQR) (Cortes-Silva et al., 2020; Hamilton et al., 2020; Nishino et al., 2012; Pesenti et al., 2018; Veld et al., 2016; Weir et al., 2016; Yan et al., 2019) allows proteins to adapt by minimizing a pathway that is exploited by a selfish element, while maintaining kinetochore function via other pathways.

Consistent with this idea of independent modules for kinetochore formation, CENP-A depletion leads to proportional reduction of centromeric CENP-C, whereas CENP-T and CENP-I persist longer (Fachinetti et al., 2013). In addition, recurrent changes in kinetochore modules are observed throughout eukaryotic evolution, such as changes in the number of MELT motifs in KNL1 and replacement of the SKA complex by the DAM complex (Hooff et al., 2017; Tromer et al., 2015). Regulation of kinetochore-microtubule attachment stability may be another way to suppress selfish genetic elements, as MELT motifs recruit BUB1 and SKA and DAM complexes stabilize attachments. Thus, internal conflicts between selfish genetic elements and the chromosome segregation machinery may have shaped complexity in eukaryotic centromeres.

## Limitations of the Study

Although we are able to experimentally weaken the kinetochore pathway specifically by rat CENP-C expression, we are unable to reduce heterochromatin without also perturbing the kinetochore pathway. Functional changes in heterochromatin likely require manipulations on longer timescales than the typical microinjection experiment, so testing possible experimental strategies will require transgenic or genome-edited animals. Given this limitation, our results imply that the dominant effect of CENP-B deletion is to weaken the heterochromatin pathway, as explained in the Results section. Alternatively, CENP-B may equalize centromeres through an uncharacterized pathway independent of kinetochore assembly and heterochromatin, to explain our finding that CENP-B deletion increases functional asymmetry.

## STAR Methods

### RESOURCE AVAILABILITY

**Lead Contact**—Further information and requests for resources and reagents should be directed to and will be fulfilled by the Lead Contact, Michael A. Lampson (lampson@sas.upenn.edu).

**Materials Availability**—Plasmids generated in this study will be available from Addgene (Michael Lampson Lab Plasmids).

### Data and Code Availability

- The draft genomes and raw sequencing reads have been submitted to the NCBI BioProject database (<https://www.ncbi.nlm.nih.gov/bioproject>) under accession number PRJNA669840. Raw imaging data is available from the authors upon request.
- In-house scripts and pipelines are deposited to GitHub ([https://github.com/TomoKumon/Kumon\\_Cell\\_2021](https://github.com/TomoKumon/Kumon_Cell_2021)) with DOI 10.5281/zenodo.5129774.
- Any additional information required to reanalyze the data reported in this work paper is available from the Lead Contact upon request.

## EXPERIMENTAL MODEL AND SUBJECT DETAILS

**Mice**—Mouse strains were purchased from the Jackson Laboratory (ZALENDE/EiJ, stock #001392 corresponds to CHPO; C57BL/6J, stock# 000664) and from Envigo (NSA, stock# 033 corresponds to CF-1). CHPO males were crossed to CF-1 females to generate hybrids shown in Figure 1C and Supplementary Figure 1B. The CHPO strain contains seven Robertsonian fusions (Rb(1.3), Rb(4.6), Rb(5.15), Rb(11.13), Rb(8.12), Rb(9.14), and Rb(16.17)), each of which pairs with two CF-1 chromosomes in CHPO hybrid meiosis I to form a trivalent (Chmátal et al., 2014). We included only bivalents (chromosome 2, 7, 10, 18, 19, X) in our analyses to avoid complications of trivalents.

In order to generate CENP-B null mice, 1-cell embryos (from female CF-1 and male DBA/2J × C57BL/6J hybrid) were collected and microinjected with Cas9 mRNA (TriLink, CleanCap Cas9 mRNA, L-7606) and gRNA (GAAGAACAAGCGCGCCA) (Thermo Fisher scientific, GeneArt Precision gRNA Synthesis Kit, A29377). Embryos were cultured *in vitro* until blastocyst stage and transferred to pseudopregnant females to produce a founder mouse carrying 37bp deletion (TGAGCACCATCCTGAAGAACAAGCGCGCCATCCTGGC) that produces a premature stop codon at Leu100 in the DNA binding domain. The founder was crossed with C57BL/6J for multiple generations to remove possible off-target mutations. Mice were genotyped by extracting genomic DNA from tail clip (QIAGEN, DNeasy Blood & Tissue Kit, 69504) and amplifying a *Cenpb* fragment (Agilent, Herculase II Fusion DNA Polymerase). To generate *Cenpb* null mice with larger and smaller centromeres, CHPO females were crossed to C57BL/6J *Cenpb* null males to generate first generation hybrid females, which were then crossed to C57BL/6J *Cenpb* null males to generate second-generation hybrid females as shown in Figure 3B and Supplementary Figure 3D. All animal experiments were approved by the Institutional Animal Care and Use Committee and were consistent with the National Institutes of Health guidelines. The age of the mice used in the study was 8–14 weeks.

## METHOD DETAILS

**Oocyte Collection and Culture**—Female mice (8–14 weeks of age) were hormonally primed with 5U of Pregnant Mare Serum Gonadotropin (PMSG, Calbiochem, cat# 367222) or 0.1mL of CARD HyperOva (Cosmo Bio, KYD-010-EX) 44–48 h prior to oocyte collection. Germinal vesicle (GV)-intact oocytes were collected in M2 medium (Sigma, M7167), denuded from cumulus cells, and cultured in Chatot-Ziomek-Bavister (CZB) medium (Thermo Fisher, MR019D) in a humidified atmosphere of 5% CO<sub>2</sub> in air at 37.8°C. During collection, meiotic resumption was inhibited by addition of 2.5 mM milrinone. Milrinone was subsequently washed out to allow meiotic resumption. Oocytes were checked for GVBD (germinal vesicle breakdown), and those that did not enter GVBD stage were removed from the culture.

**Oocyte Microinjection**—GV oocytes were microinjected with ~5 pl of cRNAs in M2 medium (with 2.5 mM milrinone and 3mg/mL BSA) at room temperature (RT) with a micromanipulator TransferMan NK 2 (Eppendorf) and picoinjector (Medical Systems Corp.). After the injection, oocytes were kept in milrinone for 16 h to allow protein expression. cRNAs used for microinjections were dCas9-EGFP (dead Cas9 with EGFP at

the N terminus) at 1000ng/μL, dCas9-mCherry (dead Cas9 with mCherry at the N terminus) at 1000ng/μL, gRNA that targets minor satellite repeat (ACACTGAAAAACACATTCGT) at 200ng/μL, H2B-EGFP (human histone H2B with EGFP at the C terminus) at 150ng/μL, H2B-mCherry (human histone H2B with mCherry at the C terminus) at 150ng/μL, EGFP-MmCENP-C (mouse CENP-C with EGFP at the N terminus) at 100ng/μL, EGFP-RnCENP-C (rat CENP-C with EGFP at the N terminus) at 100ng/μL, and EGFP-RpCENP-C (*R. pumilio* CENP-C with EGFP at the N terminus) at 100ng/μL. Mouse, rat and *R. pumilio* CENP-C sequences were cloned from cDNA libraries from liver. Mouse and rat CENP-C sequences were verified by mm10 *Mus musculus* and rn6 *Rattus norvegicus* reference genomes. *R. pumilio* CENP-C sequence was verified by the genome sequence (personal communication with Ricardo Mallarino). cRNAs were synthesized using the T7 mScript™ Standard mRNA Production System (CELL SCRIPT) or mMESSAGING mMACHINE SP6 Transcription Kit (Thermo Fisher scientific). gRNAs were synthesized using GeneArt Precision gRNA Synthesis Kit (Thermo Fisher scientific A29377).

**Live Imaging and Chromosome Position Assay**—For the chromosome position assay, oocytes were collected and microinjected with the constructs indicated in the figure legends. After inducing meiotic resumption by washing out milrinone, oocytes were placed into 2μL drops of CZB media covered with mineral oil in a glass-bottom tissue culture dish (FluoroDish FD35–100) in a heated environmental chamber with a stage top incubator (Incubator BL and Heating Insert P; PeCon GmbH) to maintain 37°C. Confocal images were collected with a microscope (DMI4000 B; Leica) equipped with a 63× 1.3 NA glycerol-immersion objective lens, an xy piezo Z stage (Applied Scientific Instrumentation), a spinning disk confocal scanner (Yokogawa Corporation of America), and an electron multiplier charge-coupled device camera (ImageEM C9100–13; Hamamatsu Photonics), controlled by MetaMorph software (Molecular Devices). Excitation was with an LMM5 laser merge module with 488- and 593-nm lasers (Spectral Applied Research) or a Vortran Stradus VersaLase 4 laser module with 405 nm, 488 nm, 561 nm, and 639 nm lasers (Vortran Laser Technology). Confocal images were collected as z stacks at 0.5 μm intervals to visualize the entire meiotic spindle. The position of the spindle near the cortex was confirmed by differential interference contrast images. The spindle equator was determined as a middle of the spindle. The chromosome position of each bivalent was determined as a crossover site and normalized by the distance between spindle equator and spindle poles.

**Oocyte Immunocytochemistry**—After inducing meiotic resumption by washing out milrinone (4.5 hours for prometaphase staining and 7.5 hours for metaphase staining), MI oocytes were fixed in freshly prepared 2% paraformaldehyde in PBS with 0.1% Triton X-100, pH 7.4, for 20 min at RT, permeabilized in PBS with 0.1% Triton X-100 for 15 min at RT, placed in blocking solution (PBS containing 0.3% BSA and 0.01% Tween-20) 15 min RT or overnight at 4C, incubated 1–2 h with primary antibodies in blocking solution, washed 3 times for 15 min each, incubated 1 h with secondary antibodies, washed 3 times for 15 min each, and mounted in Vectashield with DAPI (Vector, H-1200) to visualize chromosomes. Primary antibodies used for this study were rabbit anti-human H3K9me3 (1:500; Abcam, ab8898), mouse anti-mouse SGO2 (1:500, a gift from Yoshinori Watanabe), and rabbit anti-mouse CENP-C (1:2500, a gift from Yoshinori Watanabe). Secondary antibodies were

Alexa Fluor 488–conjugated donkey anti-rabbit or donkey anti-mouse, Alexa Fluor 594–conjugated donkey anti-rabbit or donkey anti-mouse, or Alexa Fluor 647–conjugated donkey anti-rabbit or donkey anti-mouse (1:500, Invitrogen). Confocal images were collected as z stacks at 0.5  $\mu\text{m}$  intervals to visualize the entire meiotic spindle, using the spinning disc confocal microscope described above. To quantify centromere signal ratios, optical slices containing centromeres from the same bivalent were added to produce a sum projection using Fiji/ImageJ. Ellipses were drawn around the centromeres, and signal intensity was integrated over each ellipse after subtracting cytoplasmic background. Ratios were obtained for each bivalent by dividing the intensity of the larger centromere by that of the smaller centromere, as determined by dCas9 signal intensity.

**Whole Genome Sequencing of Six Murinae Species**—Frozen tissue samples from male individuals were obtained from the Museum of Vertebrate Zoology, Berkeley, CA (MZV) and the Field Museum of Natural History, Chicago, IL (FMNH). *Hylomyscus alleni* (MVZ Mamm 196246) was captured in Cameroon in 2000, *Praomys delectorum* (MVZ Mamm 221157) was captured in Malawi in 2007, *Mastomys natalensis* (MVZ Mamm 221054) was captured in Malawi in 2007, *Grammomys dolichurus* (MVZ Mamm 221001) was captured in Malawi in 2007, *Rhabdomys dilectus* (FMNH 192475) was captured in Malawi in 2006, and *Rhynchomys soricoides* (FMNH 198792) was captured in The Philippines in 2008. All genomes were sequenced in the Center for Applied Genomics at Children’s Hospital of Philadelphia. High molecular weight DNA was extracted following the protocol provided by 10xGenomics (CG000072 Rev B Sample Preparation Demonstrated Protocol, DNA Extraction from Fresh Frozen Tissue). Extracted DNA was quality controlled (CG00019 Rev B Sample Preparation Demonstrated Protocol, High Molecular Weight DNA QC), and all of the samples had a mean length greater than 50kb, and high enough concentration to dilute to 1ng/ $\mu\text{L}$  for library preparation. Chromium Genome Reagent Kits v2 from 10xGenomics was used to prepare libraries of 2 $\times$ 150 base reads, with read 1 constituting 10xBarcode (16bp) + nmer (6bp) + genome sequence (128bp) and read 2 constituting genome sequence (150bp). i7 index used 8bp sample index, and i5 index was not used. Sequencing depth was calculated based on putative genome size 3Gb and coverage 56x, following 10xGenomics R&D recommendation, and the libraries were sequenced with Illumina HiSeq. Demultiplexed FASTQ files were analyzed using the LongRanger wgs -basic pipeline. This pipeline gave general QC statistics related to the 10x barcoding and number of read pairs present in the FASTQ files. All sample FASTQs contained more than 688M read pairs and have acceptable barcode diversity/% on whitelist. LongRanger was used to assemble genomes, using the *Mus musculus* (mm10) as reference. In parallel, Supernova was used to assemble *de novo* genomes. See Supplementary Table 1 for assembly statistics. In order to obtain protein coding sequences, mm10 annotation was used to annotate reference-guided assemblies, and translated BLAST (tblastn) was used to pull homologous sequences from de novo assemblies using *Mus musculus* protein sequences as query sequences.

**Phylogenetic Tree Construction**—The species tree shown in Figure 4B was obtained from maximum likelihood (RAxML) and Bayesian inference (MrBayes). The phylogeny within *Mus* was previously studied (Keane et al., 2011; Thybert et al., 2018). In order



to resolve phylogeny in Murinae, the same set of genes that were used to construct a primate phylogenetic tree (Perelman et al., 2011) was aligned by MAFFT (Kato and Standley, 2013; Kato et al., 2002). The initial alignment was imported in Geneious Prime, and manually inspected for sequence alignment ambiguity. Ambiguous regions were removed from subsequent analyses. Maximum likelihood tree was constructed with RAxML (Stamatakis, 2014), and Bayesian inference tree was constructed with MrBayes (Huelsenbeck and Ronquist, 2001), with *Peromyscus maniculatus* as outgroup. Both inferences supported the tree topology shown in Figure 4B.

**Molecular Evolution Analyses**—In order to create a histogram in Figure 4C, alignments of mouse-rat orthologs were filtered for dS below 0.5, as higher dS values indicate misalignment. A list of genes for each subcellular compartment was obtained from Human Protein Atlas. Mouse-human orthologs were used to calculate average dN/dS for each subcellular compartment in Figure 4D. The analysis to identify signatures of positive selection (PAML) is highly sensitive to alignment errors, so automated genome-wide analysis is prone to false positives (van der Lee et al., 2017). To prevent these errors, alignments for selected genes were manually inspected. Coding sequences for each gene were aligned by Geneious Alignment (translation align) implemented in Geneious Prime, and manually inspected for sequence alignment ambiguity. Insertions or deletions as well as their flanking codons were removed from analyses. To test signatures of positive selection, we compared the likelihood of models of neutral codon evolution to models of codon evolution allowing positive selection, implemented in PAML version 4 (Yang, 2007). The neutral model M1 (fixed dN/dS values between 0 to 1) and M2 (M1 parameters plus dN/dS > 1) were compared in the first test, and the neutral model M7 (dN/dS values fit a beta distribution from 0 to 1) and M8 (M7 parameters plus dN/dS > 1) were compared in the second test, assuming the F3×4 model of codon frequencies. Degree of freedom for each test was 2, and the log likelihood test was significant above 5.99 ( $p < 0.05$ ). We first used the species tree, and signatures of positive selection were confirmed using a gene tree for each gene, created by RAxML.

## QUANTIFICATION AND STATISTICAL ANALYSIS

Data points are pooled from at least two independent experiments. The following statistical methods were used: unpaired t test in Figures 2B, 2C, 2D, 2E, 2G, 2I, 3A, 3C, 3D, S1D, S1G, S1H, S3E, and S3F; Mann-Whitney U test in Figure 4D; ordinary one-way ANOVA in Figure S1D; chi square test for goodness of fit for deviations from 1 in Figure 1D and for statistical models (likelihood-ratio test) in Figure 4E and Supplementary Table 2; Naïve Empirical Bayes (NEB) analysis and Bayes Empirical Bayes (BEB) analysis in Figures 4B and 4E; F test to compare variance in Figure S5C. The exact value of n, what n represents, and definition of center can be found in the figure legends for each experiment. Unpaired t test, Mann-Whitney U test, ordinary one-way ANOVA, and F test were performed using GraphPad Prism; chi square tests were performed using Excel; NEB and BEB analyses were performed using PAML model 2 and 8. *P* value of less than 0.05 was judged as statistically significant.

## Supplementary Material

Refer to Web version on PubMed Central for supplementary material.

## Acknowledgements

We thank B.E. Black for comments on the manuscript, Y. Watanabe for the CENP-C and SGO2 antibodies, R. Mallarino for *Rhabdomys pumilio* animals, J.B. Searle, C. Conroy (Museum of Vertebrate Zoology), and A. Ferguson (Field Museum of Natural History) for collecting Murinae tissue samples, K.G. Boese for assistance with the image analyses, and G. Thomas and J. Good for assistance with the genomic analyses. The research was supported by the NIH (R35GM122475 to M.A.L.; R35GM124684 to M.T.L.; RM1HG010023 to J.K.) and a predoctoral fellowship from the Funai Foundation for Information Technology (T.K.).

## References

- Abe Y, Sako K, Takagaki K, Hirayama Y, Uchida KSK, Herman JA, DeLuca JG, and Hirota T (2016). HP1-assisted Aurora B kinase activity prevents chromosome segregation errors. *Developmental Cell* 36, 487–497. [PubMed: 26954544]
- Ainsztein AM, Kandels-Lewis SE, Mackay AM, and Earnshaw WC (1998). INCENP centromere and spindle targeting: identification of essential conserved motifs and involvement of heterochromatin protein HP1. *Journal of Cell Biology* 143, 1763–1774.
- Akera T, Chmátal L, Trimm E, Yang K, Aonbangkhen C, Chenoweth DM, Janke C, Schultz RM, and Lampson MA (2017). Spindle asymmetry drives non-Mendelian chromosome segregation. *Science* 358, 668–672. [PubMed: 29097549]
- Akera T, Trimm E, and Lampson MA (2019). Molecular strategies of meiotic cheating by selfish centromeres. *Cell* 178, 1132–1144. [PubMed: 31402175]
- Allshire RC, and Madhani HD (2017). Ten principles of heterochromatin formation and function. *Nature Reviews Molecular Cell Biology* 19, 229–244. [PubMed: 29235574]
- Allu PK, Dawicki-McKenna JM, Eeuwen TV, Slavin M, Braitbard M, Xu C, Kalisman N, Murakami K, and Black BE (2019). Structure of the human core centromeric nucleosome complex. *Current Biology* 29, 2625–2639. [PubMed: 31353180]
- Amor DJ, Bentley K, Ryan J, Perry J, Wong L, Slater H, and Choo KHA (2004). Human centromere repositioning “in progress.” *Proceedings of the National Academy of Sciences* 101, 6542–6547.
- Bint SM, Ogilvie CM, Flinter FA, Khalaf Y, and Scriven PN (2011). Meiotic segregation of Robertsonian translocations ascertained in cleavage-stage embryos—implications for preimplantation genetic diagnosis. *Human Reproduction* 26, 1575–1584. [PubMed: 21441546]
- Casola C, Hucks D, and Feschotte C (2007). Convergent domestication of pogo-like transposases into centromere-binding proteins in fission yeast and mammals. *Molecular Biology and Evolution* 25, 29–41. [PubMed: 17940212]
- Cazaux B, Catalan J, Justy F, Escudé C, Desmarais E, and Britton-Davidian J (2013). Evolution of the structure and composition of house mouse satellite DNA sequences in the subgenus *Mus* (Rodentia: Muridea): a cytogenomic approach. *Chromosoma* 122, 209–220. [PubMed: 23515652]
- Cheerambathur DK, Prevo B, Chow T-L, Hattersley N, Wang S, Zhao Z, Kim T, Gerson-Gurwitz A, Oegema K, Green R, et al. (2019). The kinetochore-microtubule coupling machinery is repurposed in sensory nervous system morphogenesis. *Developmental Cell* 48, 864–872. [PubMed: 30827898]
- Chen L, Qiu Q, Jiang Y, Wang K, Lin Z, Li Z, Bibi F, Yang Y, Wang J, Nie W, et al. (2019). Large-scale ruminant genome sequencing provides insights into their evolution and distinct traits. *Science* 364, eaav6202.
- Chmátal L, Gabriel SI, Mitsainas GP, Martínez-Vargas J, Ventura J, Searle JB, Schultz RM, and Lampson MA (2014). Centromere strength provides the cell biological basis for meiotic drive and karyotype evolution in mice. *Current Biology* 24, 2295–2300. [PubMed: 25242031]
- Chmátal L, Yang K, Schultz RM, and Lampson MA (2015). Spatial regulation of kinetochore microtubule attachments by destabilization at spindle poles in meiosis I. *Current Biology* 25, 1835–1841. [PubMed: 26166779]

- Cortes-Silva N, Ulmer J, Kiuchi T, Hsieh E, Cornilleau G, Ladid I, Dingli F, Loew D, Katsuma S, and Drinnenberg IA (2020). CenH3-independent kinetochore assembly in Lepidoptera requires CCAN, including CENP-T. *Current Biology* 30, 561–572. [PubMed: 32032508]
- Dambacher S, Deng W, Hahn M, Sadic D, Fröhlich J, Nuber A, Hoischen C, Diekmann S, Leonhardt H, and Schotta G (2012). CENP-C facilitates the recruitment of M18BP1 to centromeric chromatin. *Nucleus* 3, 101–110. [PubMed: 22540025]
- Daniel A (2002). Distortion of female meiotic segregation and reduced male fertility in human Robertsonian translocations: Consistent with the centromere model of co-evolving centromere DNA/centromeric histone (CENP-A). *American Journal of Medical Genetics* 111, 450–452. [PubMed: 12210311]
- Diaz-Rodriguez E, Sotillo R, Schwartzman J-M, and Benezra R (2008). Hec1 overexpression hyperactivates the mitotic checkpoint and induces tumor formation in vivo. *Proceedings of the National Academy of Sciences* 105, 16719–16724.
- Dunleavy EM, Roche D, Tagami H, Lacoste N, Ray-Gallet D, Nakamura Y, Daigo Y, Nakatani Y, and Almouzni-Pettinotti G (2009). HJURP is a cell-cycle-dependent maintenance and deposition factor of CENP-A at centromeres. *Cell* 137, 485–497. [PubMed: 19410545]
- Echave J, Spielman SJ, and Wilke CO (2016). Causes of evolutionary rate variation among protein sites. *Nature Reviews Genetics* 17, 109–121.
- Fachinetti D, Folco HD, Nechemia-Arbely Y, Valente LP, Nguyen K, Wong AJ, Zhu Q, Holland AJ, Desai A, Jansen LET, et al. (2013). A two-step mechanism for epigenetic specification of centromere identity and function. *Nature Cell Biology* 15, 1056–1066. [PubMed: 23873148]
- Fachinetti D, Han JS, McMahon MA, Ly P, Abdullah A, Wong AJ, and Cleveland DW (2015). DNA sequence-specific binding of CENP-B enhances the fidelity of human centromere function. *Developmental Cell* 33, 314–327. [PubMed: 25942623]
- Finseth FR, Dong Y, Saunders A, and Fishman L (2015). Duplication and adaptive evolution of a key centromeric protein in *Mimulus*, a genus with female meiotic drive. *Molecular Biology and Evolution* 32, 2694–2706. [PubMed: 26104011]
- Finseth FR, Nelson TC, and Fishman L (2021). Selfish chromosomal drive shapes recent centromeric histone evolution in monkeyflowers. *PLOS Genetics* 17, e1009418. [PubMed: 33886547]
- Fishman L, and Saunders A (2008). Centromere-associated female meiotic drive entails male fitness costs in monkeyflowers. *Science* 322, 1559–1562. [PubMed: 19056989]
- Foltz DR, Jansen LET, Bailey AO, Yates JR, Bassett EA, Wood S, Black BE, and Cleveland DW (2009). Centromere-specific assembly of CENP-A nucleosomes is mediated by HJURP. *Cell* 137, 472–484. [PubMed: 19410544]
- Fujita Y, Hayashi T, Kiyomitsu T, Toyoda Y, Kokubu A, Obuse C, and Yanagida M (2007). Priming of centromere for CENP-A recruitment by human hMis18 $\alpha$ , hMis18 $\beta$ , and M18BP1. *Developmental Cell* 12, 17–30.
- Gamba R, and Fachinetti D (2020). From evolution to function: Two sides of the same CENP-B coin? *Experimental Cell Research* 390, 111959. [PubMed: 32173469]
- Gao B, Wang Y, Diaby M, Zong W, Shen D, Wang S, Chen C, Wang X, and Song C (2020). Evolution of pogo, a separate superfamily of IS630-Tc1-mariner transposons, revealing recurrent domestication events in vertebrates. *Mobile DNA* 11, 25. [PubMed: 32742312]
- Gibbs RA, Weinstock GM, Metzker ML, Muzny DM, Sodergren EJ, Scherer S, Scott G, Steffen D, Worley KC, Burch PE, et al. (2004). Genome sequence of the Brown Norway rat yields insights into mammalian evolution. *Nature* 428, 493–521. [PubMed: 15057822]
- Godek KM, Kabeche L, and Compton DA (2014). Regulation of kinetochore-microtubule attachments through homeostatic control during mitosis. *Nature Reviews Molecular Cell Biology* 16, 57–64. [PubMed: 25466864]
- Hamilton GE, Helgeson LA, Noland CL, Asbury CL, Dimitrova YN, and Davis TN (2020). Reconstitution reveals two paths of force transmission through the kinetochore. *eLife* 9, e56582. [PubMed: 32406818]
- Hemmerich P, Weidtkamp-Peters S, Hoischen C, Schmiedeberg L, Erliandri I, and Diekmann S (2008). Dynamics of inner kinetochore assembly and maintenance in living cells. *Journal of Cell Biology* 180, 1101–1114.

- Henikoff S, Ahmad K, and Malik HS (2001). The centromere paradox: stable inheritance with rapidly evolving DNA. *Science* 293, 1098–1102. [PubMed: 11498581]
- Higgins JMG, and Prendergast L (2016). Mitotic mysteries: the case of HP1. *Developmental Cell* 36, 477–478. [PubMed: 26954539]
- Hooff J.J. van, Snel B, and Kops GJ (2017). Unique phylogenetic distributions of the Ska and Dam1 complexes support functional analogy and suggest multiple parallel displacements of Ska by Dam1. *Genome Biology and Evolution* 9, 1295–1303. [PubMed: 28472331]
- Hudson DF, Fowler KJ, Earle E, Saffery R, Kalitsis P, Trowell H, Hill J, Wreford NG, Kretser D.M. de, Cancelli MR, et al. (1998). Centromere protein B null mice are mitotically and meiotically normal but have lower body and testis weights. *Journal of Cell Biology* 141, 309–319.
- Huelsenbeck JP, and Ronquist F (2001). MRBAYES: Bayesian inference of phylogenetic trees. *Bioinformatics* 17, 754–755. [PubMed: 11524383]
- Iwata-Otsubo A, Dawicki-McKenna JM, Akera T, Falk SJ, Chmátal L, Yang K, Sullivan BA, Schultz RM, Lampson MA, and Black BE (2017). Expanded satellite repeats amplify a discrete CENP-A nucleosome assembly site on chromosomes that drive in female meiosis. *Current Biology* 27, 2365–2373. [PubMed: 28756949]
- Jangam D, Feschotte C, and Betrán E (2017). Transposable element domestication as an adaptation to evolutionary conflicts. *Trends in Genetics* 33, 817–831. [PubMed: 28844698]
- Javed AO, Li Y, Muffat J, Su K-C, Cohen MA, Lungjangwa T, Aubourg P, Cheeseman IM, and Jaenisch R (2018). Microcephaly modeling of kinetochore mutation reveals a brain-specific phenotype. *Cell Reports* 25, 368–382. [PubMed: 30304678]
- Kang J, Chaudhary J, Dong H, Kim S, Brautigam CA, and Yu H (2011). Mitotic centromeric targeting of HP1 and its binding to Sgo1 are dispensable for sister-chromatid cohesion in human cells. *Molecular Biology of the Cell* 22, 1181–1190. [PubMed: 21346195]
- Kapoor M, Luna R.M. de O., Liu G, Lozano G, Cummings C, Mancini M, Ouspenski I, Brinkley BR, and May GS (1998). The cenpB gene is not essential in mice. *Chromosoma* 107, 570–576. [PubMed: 9933410]
- Kato H, Jiang J, Zhou B-R, Rozendaal M, Feng H, Ghirlando R, Xiao TS, Straight AF, and Bai Y (2013). A conserved mechanism for centromeric nucleosome recognition by centromere protein CENP-C. *Science* 340, 1110–1113. [PubMed: 23723239]
- Katoh K, and Standley DM (2013). MAFFT multiple sequence alignment software version 7: improvements in performance and usability. *Molecular Biology and Evolution* 30, 772–780. [PubMed: 23329690]
- Katoh K, Misawa K, Kuma K, and Miyata T (2002). MAFFT: a novel method for rapid multiple sequence alignment based on fast Fourier transform. *Nucleic Acids Research* 30, 3059–3066. [PubMed: 12136088]
- Kawashima SA, Yamagishi Y, Honda T, Ishiguro K, and Watanabe Y (2009). Phosphorylation of H2A by Bub1 prevents chromosomal instability through localizing Shugoshin. *Science* 327, 172–177. [PubMed: 19965387]
- Keane TM, Goodstadt L, Danecek P, White MA, Wong K, Yalcin B, Heger A, Agam A, Slater G, Goodson M, et al. (2011). Mouse genomic variation and its effect on phenotypes and gene regulation. *Nature* 477, 289–294. [PubMed: 21921910]
- Kelly AE, Ghenoïu C, Xue JZ, Zierhut C, Kimura H, and Funabiki H (2010). Survivin reads phosphorylated histone H3 threonine 3 to activate the mitotic kinase Aurora B. *Science* 330, 235–239. [PubMed: 20705815]
- Kim J, Ishiguro K, Nambu A, Akiyoshi B, Yokobayashi S, Kagami A, Ishiguro T, Pendas AM, Takeda N, Sakakibara Y, et al. (2015). Meikin is a conserved regulator of meiosis-I-specific kinetochore function. *Nature* 517, 466–471. [PubMed: 25533956]
- Kipling D, and Warburton PE (1997). Centromeres, CENP-B and Tigger too. *Trends in Genetics* 13, 141–145. [PubMed: 9097724]
- Klare K, Weir JR, Basilico F, Zimniak T, Massimiliano L, Ludwigs N, Herzog F, and Musacchio A (2015). CENP-C is a blueprint for constitutive centromere-associated network assembly within human kinetochores. *Journal of Cell Biology* 210, 11–22.

- Krenn V, Overlack K, Primorac I, Gerwen S. van, and Musacchio A (2013). KI motifs of human Knl1 enhance assembly of comprehensive spindle checkpoint complexes around MELT repeats. *Current Biology* 24, 29–39. [PubMed: 24361068]
- Lampson MA, and Black BE (2017). Cellular and molecular mechanisms of centromere drive. *Cold Spring Harbor Symposia on Quantitative Biology* 82, 249–257. [PubMed: 29440567]
- Langley SA, Miga KH, Karpen GH, and Langley CH (2019). Haplotypes spanning centromeric regions reveal persistence of large blocks of archaic DNA. *eLife* 8, e42989. [PubMed: 31237235]
- Logsdon GA, Gambogi CW, Liskovych MA, Barrey EJ, Larionov V, Miga KH, Heun P, and Black BE (2019). Human artificial chromosomes that bypass centromeric DNA. *Cell* 178, 624–639. [PubMed: 31348889]
- Maheshwari S, Tan EH, West A, Franklin FCH, Comai L, and Chan SWL (2015). Naturally occurring differences in CENH3 affect chromosome segregation in zygotic mitosis of hybrids. *PLOS Genetics* 11, e1004970. [PubMed: 25622028]
- Malik HS, and Henikoff S (2001). Adaptive evolution of Cid, a centromere-specific histone in *Drosophila*. *Genetics* 157, 1293–1298. [PubMed: 11238413]
- Malik HS, and Henikoff S (2009). Major evolutionary transitions in centromere complexity. *Cell* 138, 1067–1082. [PubMed: 19766562]
- Mallarino R, Pillay N, Hoekstra HE, and Schradin C (2018). African striped mice. *Current Biology* 28, R299–R301. [PubMed: 29614283]
- Marston AL (2015). Shugoshins: tension-sensitive pericentromeric adaptors safeguarding chromosome segregation. *Molecular and Cellular Biology* 35, 634–648. [PubMed: 25452306]
- Masumoto H, Masukata H, Muro Y, Nozaki N, and Okazaki T (1989). A human centromere antigen (CENP-B) interacts with a short specific sequence in alphoid DNA, a human centromeric satellite. *Journal of Cell Biology* 109, 1963–1973.
- Melters DP, Bradnam KR, Young HA, Telis N, May MR, Ruby JG, Sebra R, Peluso P, Eid J, Rank D, et al. (2013). Comparative analysis of tandem repeats from hundreds of species reveals unique insights into centromere evolution. *Genome Biology* 14, R10. [PubMed: 23363705]
- Moree B, Meyer CB, Fuller CJ, and Straight AF (2011). CENP-C recruits M18BP1 to centromeres to promote CENP-A chromatin assembly. *Journal of Cell Biology* 194, 855–871.
- Morozov VM, Giovinazzi S, and Ishov AM (2017). CENP-B protects centromere chromatin integrity by facilitating histone deposition via the H3.3-specific chaperone Daxx. *Epigenetics Chromatin* 10, 63. [PubMed: 29273057]
- Musacchio A, and Desai A (2017). A molecular view of kinetochore assembly and function. *Biology* 6, 5.
- Nakagawa H, Lee J-K, Hurwitz J, Allshire RC, Nakayama J, Grewal SIS, Tanaka K, and Murakami Y (2002). Fission yeast CENP-B homologs nucleate centromeric heterochromatin by promoting heterochromatin-specific histone tail modifications. *Genes Development* 16, 1766–1778. [PubMed: 12130537]
- Nishino T, Takeuchi K, Gascoigne KE, Suzuki A, Hori T, Oyama T, Morikawa K, Cheeseman IM, and Fukagawa T (2012). CENP-T-W-S-X forms a unique centromeric chromatin structure with a histone-like fold. *Cell* 148, 487–501. [PubMed: 22304917]
- Nozawa R-S, Nagao K, Masuda H-T, Iwasaki O, Hirota T, Nozaki N, Kimura H, and Obuse C (2010). Human POGZ modulates dissociation of HP1alpha from mitotic chromosome arms through Aurora B activation. *Nature Cell Biology* 12, 719–727. [PubMed: 20562864]
- Ohzeki J-I, Shono N, Otake K, Martins NMC, Kugou K, Kimura H, Nagase T, Larionov V, Earnshaw WC, and Masumoto H (2016). KAT7/HBO1/MYST2 regulates CENP-A chromatin assembly by antagonizing Suv39h1-mediated centromere inactivation. *Developmental Cell* 37, 413–427. [PubMed: 27270040]
- Okada T, Ohzeki J, Nakano M, Yoda K, Brinkley WR, Larionov V, and Masumoto H (2007). CENP-B controls centromere formation depending on the chromatin context. *Cell* 131, 1287–1300. [PubMed: 18160038]
- Otake K, Ohzeki J-I, Shono N, Kugou K, Okazaki K, Nagase T, Yamakawa H, Kouprina N, Larionov V, Kimura H, et al. (2020). CENP-B creates alternative epigenetic chromatin states permissive for CENP-A or heterochromatin assembly. *Journal of Cell Science* 133, jcs243303.

- Pacchierotti F, Tiveron C, Mailhes JB, and Davisson MT (1995). Susceptibility to vinblastine-induced aneuploidy and preferential chromosome segregation during meiosis I in Robertsonian heterozygous mice. *Teratogenesis Carcinogenesis Mutagenesis* 15, 217–230.
- Pentakota S, Zhou K, Smith C, Maffini S, Petrovic A, Morgan GP, Weir JR, Vetter IR, Musacchio A, and Luger K (2017). Decoding the centromeric nucleosome through CENP-N. *eLife* 6, e33442. [PubMed: 29280735]
- Perelman P, Johnson WE, Roos C, Seuánez HN, Horvath JE, Moreira MAM, Kessing B, Pontius J, Roelke M, Rumpler Y, et al. (2011). A molecular phylogeny of living primates. *PLOS Genetics* 7, e1001342. [PubMed: 21436896]
- Perez-Castro AV, Shamanski FL, Meneses JJ, Lovato TL, Vogel KG, Moyzis RK, and Pedersen R (1998). Centromeric protein B null mice are viable with no apparent abnormalities. *Developmental Biology* 201, 135–143. [PubMed: 9740654]
- Pesenti ME, Prumbaum D, Auckland P, Smith CM, Faesen AC, Petrovic A, Erent M, Maffini S, Pentakota S, Weir JR, et al. (2018). Reconstitution of a 26-subunit human kinetochore reveals cooperative microtubule binding by CENP-OPQUR and NDC80. *Molecular Cell* 71, 923–939. [PubMed: 30174292]
- Petrovic A, Mosalaganti S, Keller J, Mattiuzzo M, Overlack K, Krenn V, Antoni AD, Wohlgemuth S, Cecatiello V, Pasqualato S, et al. (2014). Modular assembly of RWD domains on the Mis12 complex underlies outer kinetochore organization. *Molecular Cell* 53, 591–605. [PubMed: 24530301]
- Petrovic A, Keller J, Liu Y, Overlack K, John J, Dimitrova YN, Jenni S, Gerwen S. van, Stege P, Wohlgemuth S, et al. (2016). Structure of the MIS12 complex and molecular basis of its interaction with CENP-C at human kinetochores. *Cell* 167, 1028–1040. [PubMed: 27881301]
- Rago F, Gascoigne KE, and Cheeseman IM (2015). Distinct organization and regulation of the outer kinetochore KMN network downstream of CENP-C and CENP-T. *Current Biology* 25, 671–677. [PubMed: 25660545]
- Rizvi SMA, Prajapati HK, and Ghosh SK (2017). The 2 micron plasmid: a selfish genetic element with an optimized survival strategy within *Saccharomyces cerevisiae*. *Current Genetics* 64, 25–42. [PubMed: 28597305]
- Schindelin J, Arganda-Carreras I, Frise E, Kaynig V, Longair M, Pietzsch T, Preibisch S, Rueden C, Saalfeld S, Schmid B, et al. (2012). Fiji: an open-source platform for biological-image analysis. *Nature Methods* 9, 676–682. [PubMed: 22743772]
- Schneider CA, Rasband WS, and Eliceiri KW (2012). NIH Image to ImageJ: 25 years of image analysis. *Nature Methods* 9, 671–675. [PubMed: 22930834]
- Schueler MG, Swanson W, Thomas PJ, Program NCS, and Green ED (2010). Adaptive evolution of foundation kinetochore proteins in primates. *Molecular Biology and Evolution* 27, 1585–1597. [PubMed: 20142441]
- Shi L, Hu E, Wang Z, Liu J, Li J, Li M, Chen H, Yu C, Jiang T, and Su B (2016). Regional selection of the brain size regulating gene *CASC5* provides new insight into human brain evolution. *Human Genetics* 136, 193–204. [PubMed: 27878434]
- Shono N, Ohzeki J, Otake K, Martins NMC, Nagase T, Kimura H, Larionov V, Earnshaw WC, and Masumoto H (2015). CENP-C and CENP-I are key connecting factors for kinetochore and CENP-A assembly. *Journal of Cell Science* 128, 4572–4587. [PubMed: 26527398]
- Sironi M, Cagliani R, Forni D, and Clerici M (2015). Evolutionary insights into host-pathogen interactions from mammalian sequence data. *Nature Reviews Genetics* 16, 224–236.
- Stamatakis A (2014). RAxML version 8: a tool for phylogenetic analysis and post-analysis of large phylogenies. *Bioinformatics* 30, 1312–1313. [PubMed: 24451623]
- Sugimoto K, Kuriyama K, Shibata A, and Himeno M (1997). Characterization of internal DNA-binding and C-terminal dimerization domains of human centromere/kinetochore autoantigen CENP-C in vitro: role of DNA-binding and self-associating activities in kinetochore organization. *Chromosome Research* 5, 132–141. [PubMed: 9146917]
- Suzuki A, Badger BL, Wan X, DeLuca JG, and Salmon ED (2014). The architecture of CCAN proteins creates a structural integrity to resist spindle forces and achieve proper intrakinetochore stretch. *Developmental Cell* 30, 717–730. [PubMed: 25268173]

- Takeiri A, Motoyama S, Matsuzaki K, Harada A, Taketo J, Katoh C, Tanaka K, and Mishima M (2013). New DNA probes to detect aneugenicity in rat bone marrow micronucleated cells by a pan-centromeric FISH analysis. *Mutation Research* 755, 73–80. [PubMed: 23726961]
- Talbert PB, Bryson TD, and Henikoff S (2004). Adaptive evolution of centromere proteins in plants and animals. *Journal of Biology* 3, 18. [PubMed: 15345035]
- Thybert D, Roller M, Navarro FCP, Fiddes I, Streeter I, Feig C, Martin-Galvez D, Kolmogorov M, Janoušek V, Akanni W, et al. (2018). Repeat associated mechanisms of genome evolution and function revealed by the *Mus caroli* and *Mus pahari* genomes. *Genome Research* 28, 448–459. [PubMed: 29563166]
- Tromer E, Snel B, and Kops GJPL (2015). Widespread recurrent patterns of rapid repeat evolution in the kinetochore scaffold KNL1. *Genome Biology and Evolution* 7, 2383–2393. [PubMed: 26254484]
- Tsukahara T, Tanno Y, and Watanabe Y (2010). Phosphorylation of the CPC by Cdk1 promotes chromosome bi-orientation. *Nature* 467, 719–723. [PubMed: 20739936]
- van der Lee R, Wiel L, van Dam TJP, and Huynen MA (2017). Genome-scale detection of positive selection in nine primates predicts human-virus evolutionary conflicts. *Nucleic Acids Research* 45, 10634–10648. [PubMed: 28977405]
- Veld P.J.H.I. 't, Jeganathan S, Petrovic A, Singh P, John J, Krenn V, Weissmann F, Bange T, and Musacchio A (2016). Molecular basis of outer kinetochore assembly on CENP-T. *eLife* 5, e21007. [PubMed: 28012276]
- Veld P.J.H.I. 't, Volkov VA, Stender ID, Musacchio A, and Dogterom M (2019). Molecular determinants of the Ska-Ndc80 interaction and their influence on microtubule tracking and force-coupling. *eLife* 8, e49539. [PubMed: 31804178]
- Wan X, O'Quinn RP, Pierce HL, Joglekar AP, Gall WE, DeLuca JG, Carroll CW, Liu S-T, Yen TJ, McEwen BF, et al. (2009). Protein architecture of the human kinetochore microtubule attachment site. *Cell* 137, 672–684. [PubMed: 19450515]
- Wang F, Dai J, Daum JR, Niedzialkowska E, Banerjee B, Stukenberg PT, Gorbisky GJ, and Higgins JMG (2010). Histone H3 Thr-3 phosphorylation by Haspin positions Aurora B at centromeres in mitosis. *Science* 330, 231–235. [PubMed: 20705812]
- Weir JR, Faesen AC, Klare K, Petrovic A, Basilico F, Fischböck J, Pentakota S, Keller J, Pesenti ME, Pan D, et al. (2016). Insights from biochemical reconstitution into the architecture of human kinetochores. *Nature* 537, 249–253. [PubMed: 27580032]
- Yamagishi Y, Honda T, Tanno Y, and Watanabe Y (2010). Two histone marks establish the inner centromere and chromosome bi-orientation. *Science* 330, 239–243. [PubMed: 20929775]
- Yan K, Yang J, Zhang Z, McLaughlin SH, Chang L, Fasci D, Ehrenhofer-Murray AE, Heck AJR, and Barford D (2019). Structure of the inner kinetochore CCAN complex assembled onto a centromeric nucleosome. *Nature* 574, 278–282. [PubMed: 31578520]
- Yang Z (2007). PAML 4: phylogenetic analysis by maximum likelihood. *Molecular Biology and Evolution* 24, 1586–1591. [PubMed: 17483113]
- Yang P, Wang Y, and Macfarlan TS (2017). The role of KRAB-ZFPs in transposable element repression and mammalian evolution. *Trends in Genetics* 33, 871–881. [PubMed: 28935117]
- Yao Y, and Dai W (2012). Shugoshins function as a guardian for chromosomal stability in nuclear division. *Cell Cycle* 11, 2631–2642. [PubMed: 22732496]
- Zhao G, Oztan A, Ye Y, and Schwarz TL (2019). Kinetochore proteins have a post-mitotic function in neurodevelopment. *Developmental Cell* 48, 873–882. [PubMed: 30827899]

**Highlights**

- Parallel pathways recruit drive effector proteins in a hybrid mouse model.
- Disrupting the kinetochore pathway makes centromeres functionally more similar.
- Disrupting the heterochromatin pathway makes centromeres functionally more different.
- Molecular evolution analyses show recurrent changes in both pathways.



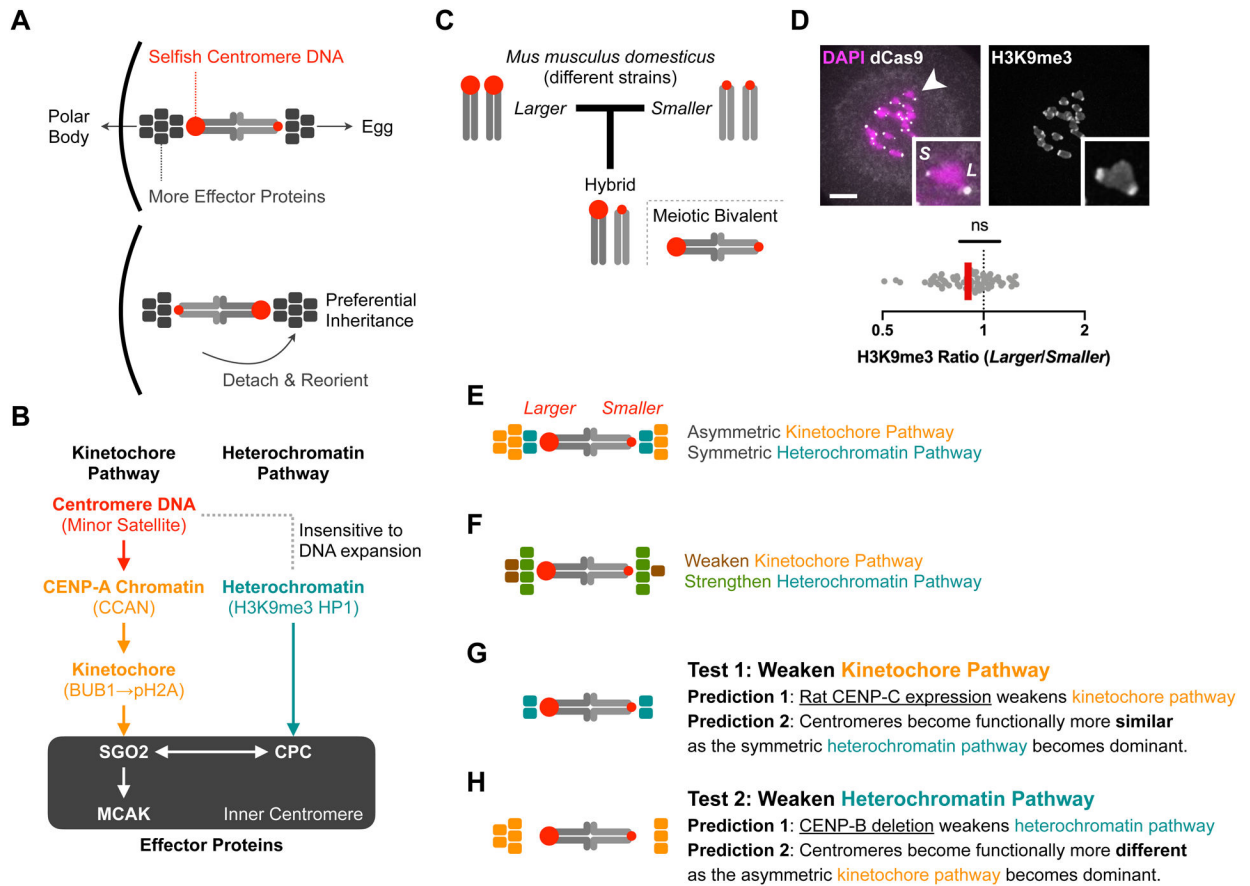


**Figure 1: Parallel pathway model for centromere drive and suppression.**

(A) Centromere drive by recruiting effector proteins that destabilize interactions with spindle microtubules. Selfish centromeres recruit more inner centromere effector proteins, preferentially detach from microtubules when facing the cortical side of the spindle, and reorient to bias their segregation to the egg. The cortical side of a meiotic bivalent will segregate to the polar body, whereas the other side will segregate to the egg.

(B) Two pathways for effector recruitment. CENP-A and the CCAN (constitutive centromere-associated network) connect centromere DNA to the kinetochores, which assembles during meiosis or mitosis. Kinetochores-localized BUB1 kinase phosphorylates pericentromeric histone H2A to recruit SGO2. In parallel, pericentromeric heterochromatin also recruits SGO2 via the CPC (chromosome passenger complex) at the inner centromere. The two pathways are not completely independent, as the CPC is also recruited by SGO2 via the kinetochores pathway. Heterochromatin appears insensitive to selfish centromere DNA expansion (see panel D).

(C) CHPO hybrid model system. Crossing strains with larger (CF-1) and smaller (CHPO) centromeres generates a hybrid in which genetically different centromeres are paired in meiotic bivalents. Larger red circles indicate more minor satellite centromere DNA repeats.

(D) CHPO hybrid oocytes were microinjected with cRNA for dCas9-EGFP and gRNA targeting minor satellite centromere DNA to distinguish larger (L) and smaller (S) centromeres, fixed at meiosis I, and stained for H3K9me3; 10 $\mu$ m scale bar, 7.4 $\mu$ m square

inset. The H3K9me3 ratio for each pair of larger and smaller centromeres within a bivalent is plotted (n=67 bivalents); red line, geometric mean; ns: no significant deviation from 1.

(E) Asymmetric kinetochore pathway and symmetric heterochromatin pathway in our hybrid model system. Colored boxes represent effector proteins recruited by the kinetochore pathway (orange) or the heterochromatin pathway (green).

(F) Suppression of functional differences between centromeres by recruiting similar amounts of effector proteins on genetically different centromeres. Colored boxes represent changes relative to panel E. Proteins in the kinetochore pathway can adapt by reducing affinity for DNA or for other proteins leading to effector recruitment. Inner centromere proteins can adapt by increasing affinity for heterochromatin or by decreasing their recruitment by the kinetochore pathway.

(G) Introducing a divergent allele of CENP-C (blue boxes) disrupts interactions for effector recruitment and therefore weakens the kinetochore pathway (prediction 1) and makes centromeres functionally more similar (prediction 2).

(H) As CENP-B recruits heterochromatin proteins, deleting CENP-B weakens the heterochromatin pathway (prediction 1), making the asymmetric kinetochore pathway dominant and centromeres functionally more asymmetric (prediction 2).

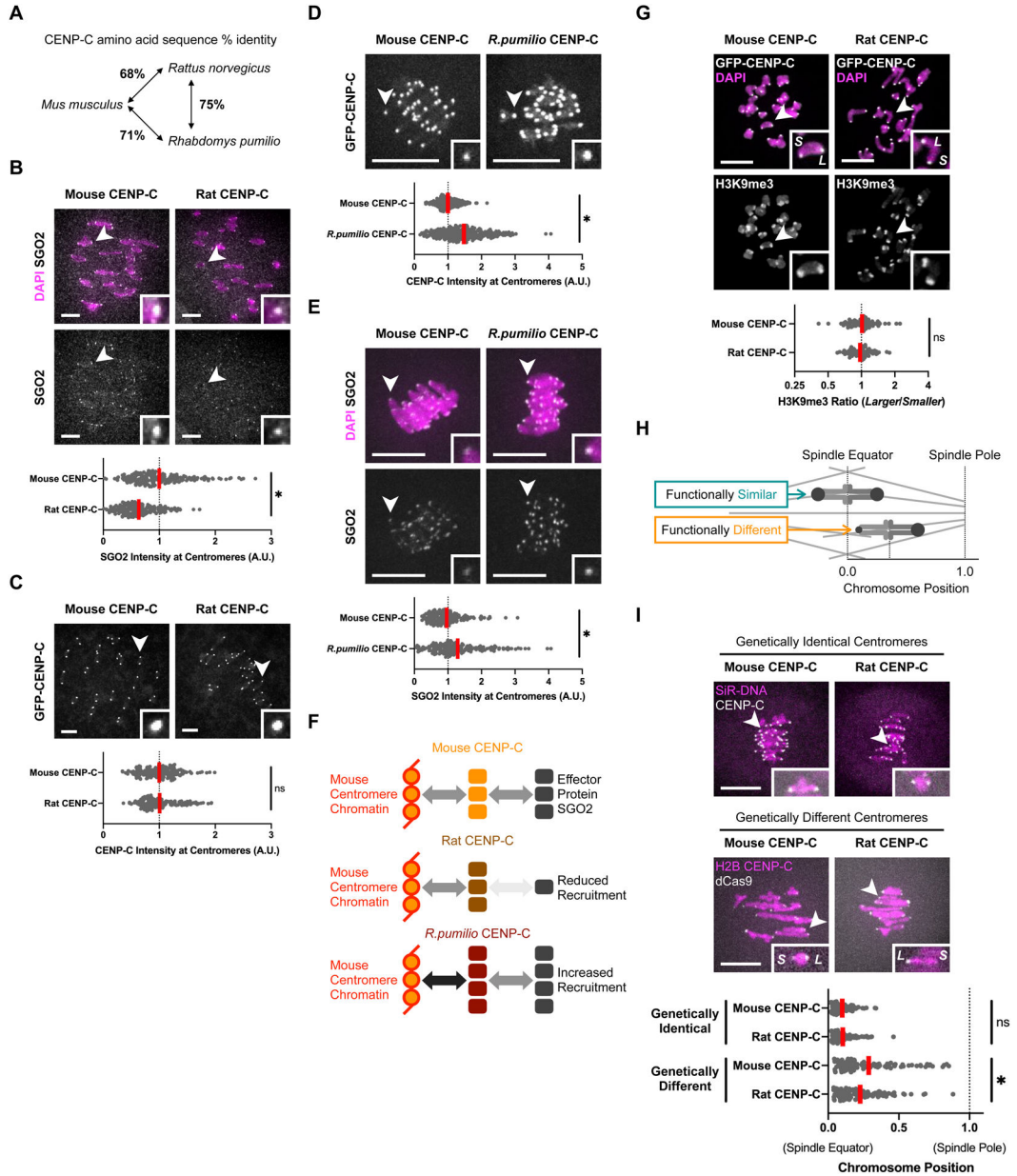


**Figure 2: Introducing rat CENP-C in mouse oocytes weakens the kinetochore pathway and makes centromeres functionally more symmetric.**

(A) CENP-C divergence between *Mus musculus* (mouse), *Rattus norvegicus* (rat), and *Rhabdomys pumilio* (a model organism closely related to *Rhabdomys dilectus*, Figure 4B). (B and C) CF-1 oocytes were microinjected with cRNA for GFP-tagged mouse or rat CENP-C and fixed in prometaphase/metaphase I. Cells were stained for SGO2 (A) or analyzed for GFP fluorescence (B). 10µm scale bars, 2.2µm square insets. Plots show centromere signal intensities. Each dot represents a single centromere (n=200 centromeres from 20 oocytes for each construct); red line, mean; \*p<0.05; ns: not significant. (D and E) CF-1 oocytes were microinjected with cRNA for GFP-tagged mouse or *R. pumilio* CENP-C and fixed in prometaphase/metaphase I. Cells were analyzed for GFP fluorescence (D) or stained for SGO2 (E). 10µm scale bars, 2.2µm square insets. Plots show

centromere signal intensities. Each dot represents a single centromere (n = 170 centromeres from 22 oocytes for each construct); red line, mean.

(F) Different CENP-C interfaces have changed to modulate effector recruitment. Schematics summarize the results of panels B to E. Compared to mouse CENP-C, rat CENP-C is similarly recruited to mouse centromere chromatin, but downstream effector recruitment is reduced. In contrast, *R. pumilio* CENP-C is recruited at higher levels to mouse centromere chromatin, leading to increased effector recruitment.

(G) CHPO hybrid oocytes (see Figure 1C) were microinjected with cRNA for GFP-tagged mouse or rat CENP-C, fixed in prometaphase/metaphase I, and stained for H3K9me3; 10µm scale bar, 5.9µm square inset. The H3K9me3 ratio for each pair of larger (*L*) and smaller (*S*) centromeres on a bivalent is plotted (n = 72 bivalents for each genotype); red line, geometric mean; ns: not significant.

(H) Schematic of chromosome position assay to measure functional differences between paired centromeres. Distance from the spindle pole to the equator is defined as 1 for each cell to normalize for variation in spindle size.

(I) For genetically identical centromeres, CF-1 oocytes were microinjected with cRNA for GFP-tagged mouse or rat CENP-C, and DNA was visualized with SiR-DNA. For genetically different centromeres, CHPO hybrid oocytes were microinjected with cRNA for GFP-tagged mouse or rat CENP-C, together with cRNAs for GFP-tagged H2B and mCherry-tagged dCas9 and gRNA targeting minor satellite centromere DNA. Cells were imaged live to preserve chromosome positions, measured at late metaphase I. In the plot, each dot represents a single bivalent (n=100 bivalents from 10 CF-1 oocytes and 20 CHPO hybrid oocytes for each construct); red line, mean.

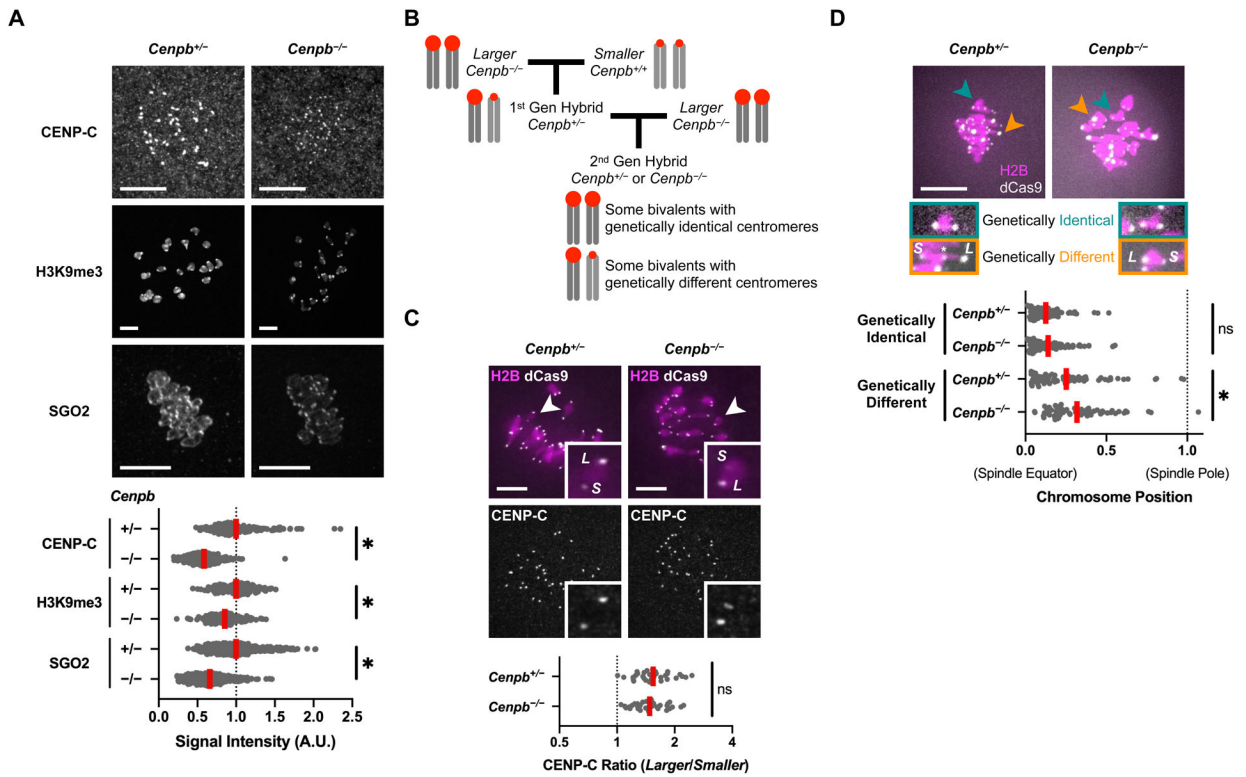


**Figure 3: Deleting CENP-B weakens the heterochromatin pathway and makes centromeres functionally more asymmetric.**

(A) *Cenpb*<sup>+/+</sup> or *Cenpb*<sup>-/-</sup> oocytes were fixed in prometaphase/metaphase of meiosis I and stained for CENP-C, H3K9me3, or SGO2; 10 $\mu$ m scale bar. Plot shows centromere signal intensities, normalized by mean intensity of *Cenpb*<sup>+/+</sup> control for each protein. Each dot represents a single centromere (n = 154 centromeres for each condition); red line, mean; \*p<0.05.

(B) Crossing scheme to produce second-generation hybrid *Cenpb*<sup>-/-</sup> mice. Oocytes from these mice have bivalents with genetically identical centromeres as well as bivalents with genetically different centromeres.

(C) Second-generation hybrid oocytes were microinjected with cRNA for dCas9-EGFP and gRNA targeting minor satellite centromere DNA, fixed in prometaphase/metaphase I, and stained for CENP-C; 10 $\mu$ m scale bar, 5.9 $\mu$ m square inset. The CENP-C ratio is plotted for each pair of larger (L) and smaller (S) centromeres on bivalents with genetically different centromeres, determined from dCas9-EGFP signals (n=34 bivalents for each genotype); red line, geometric mean; ns: not significant.

(D) Second-generation hybrid oocytes were microinjected with cRNAs for dCas9-EGFP and H2B and gRNA targeting minor satellite centromere DNA. Cells were imaged live to preserve chromosome positions, measured at late metaphase I. In the plot, each dot represents a single bivalent (n = 74 bivalents for each genotype) with either genetically identical or genetically different centromeres, determined from dCas9-EGFP signals; red line, mean.

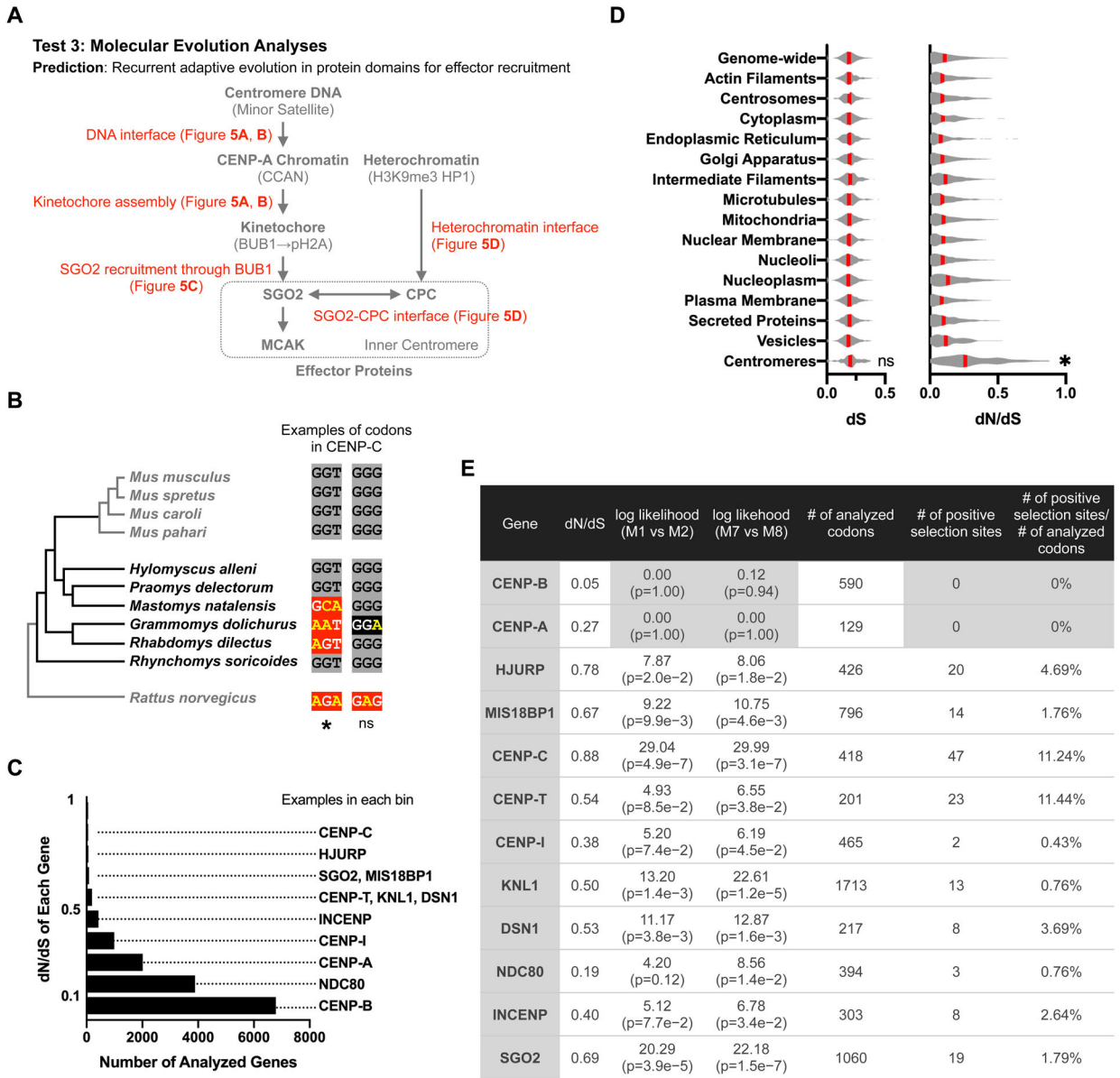


**Figure 4: Proteins in the kinetochore and heterochromatin pathways have signatures of recurrent adaptive evolution.**

(A) Our parallel pathway model predicts that proteins in both pathways will have signatures of recurrent adaptive evolution at interfaces (shown in red) that lead to effector recruitment.

(B) Phylogenetic tree of Murinae species shows previously available genomes in gray and our sequenced genomes in black. Example codons show positive selection or neutral changes (mouse CENP-C Gly469 and Gly470). Nucleotide substitutions are shown in yellow, with synonymous and nonsynonymous substitutions highlighted in black or red, respectively. Higher numbers of nonsynonymous substitutions are interpreted as adaptive change under positive selection. PAML analysis: \*P>0.99 for positive selection or not significant (ns) indicating a neutral change.

(C) Histogram shows the number of genes in each bin of dN/dS values, with examples of genes in each bin.

(D) Average dS and dN/dS across subcellular compartments. Red line, median; \* $p < 0.05$  for comparison to all other compartments.

(E) To test for signatures of positive selection in PAML, the likelihood of models of neutral codon evolution (M1 or M7) are compared to models allowing positive selection (M2 or M8). CENP-A and CENP-B are examples of genes without signatures of positive selection. See Supplementary Table 2 for other genes, Supplementary Figure 4 for a schematic of centromere proteins grouped by functional modules, and Supplementary Figure 5 for further analyses of CENP-A and CENP-B. The number of analyzed codons is less than the total protein length as insertions, deletions, and ambiguous alignments are not analyzed. The number of positive selection sites is the number of codons with  $P > 0.90$  from Naive Empirical Bayes (NEB) analysis or Bayes Empirical Bayes (BEB) analysis from model 2 or 8.

Author Manuscript

Author Manuscript

Author Manuscript

Author Manuscript

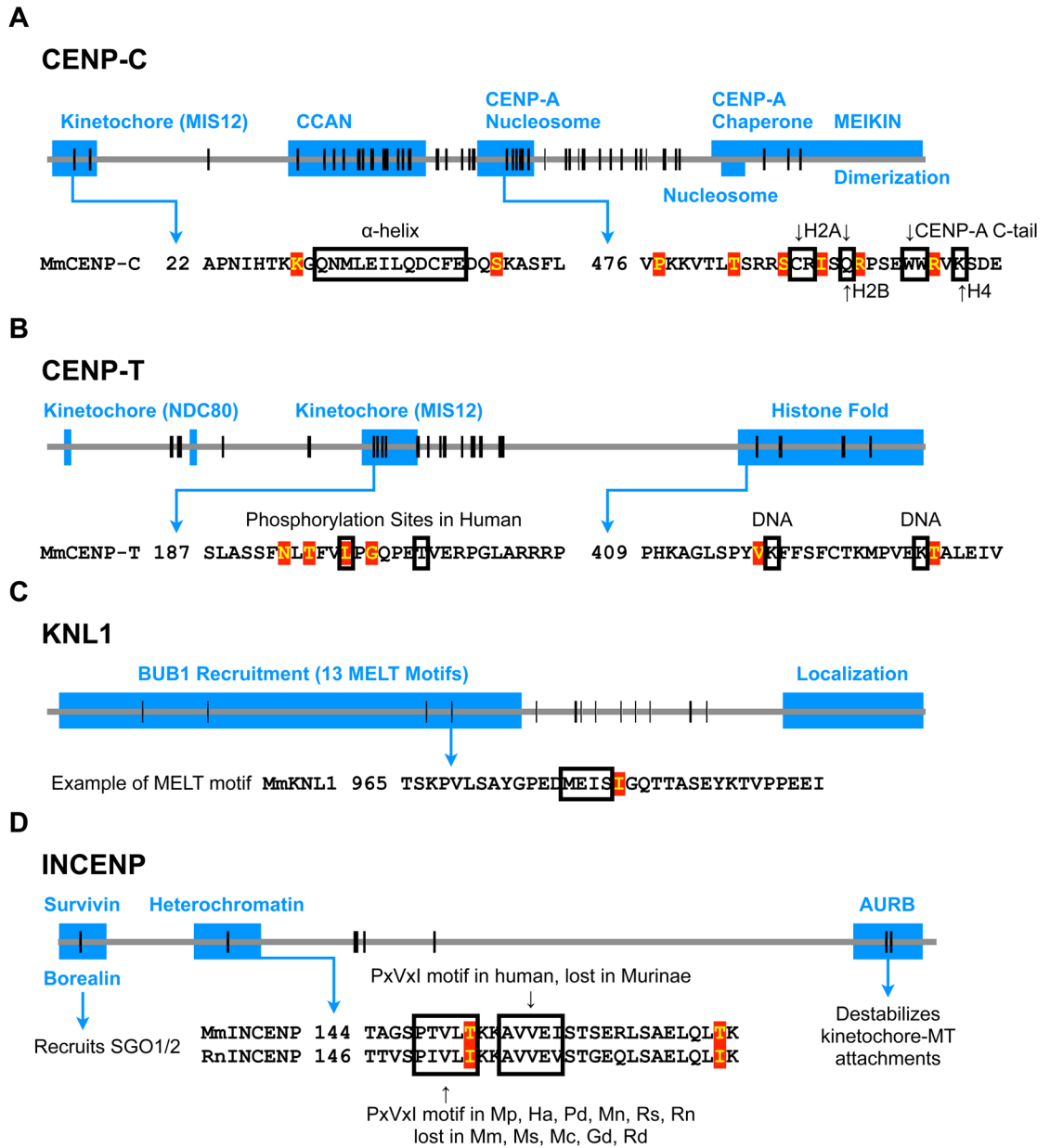


**Figure 5: Protein domains that lead to microtubule destabilizer recruitment are recurrently evolved.**

Each horizontal line represents the entire protein for each gene, and vertical lines represent positions of positively selected amino acids. Blue boxes show known functional domains from previous studies. Amino acid sequences within domains of interest are shown, with positively selected residues highlighted in red and known functional residues outlined in black.

(A) Signatures of positive selection are found throughout CENP-C. In the kinetochore domain, the α-helix interacts with MIS12 (Petrovic et al., 2016). The CCAN domain (also known as PEST domain) interacts with CENP-HIKM (Klare et al., 2015) and CENP-LN (Pentakota et al., 2017), and together forms the CENP-ACHIKMLN complex (Weir et al., 2016). In the domain interacting with CENP-A nucleosomes (also known as central region),



residues interacting with H2A, H2B, H4 and the CENP-A C-terminal tail are indicated. This domain binds CENP-A nucleosomes more specifically than the more C-terminal nucleosome binding domain (also known as CENP-C motif), which also interacts with H3 nucleosomes (Allu et al., 2019; Kato et al., 2013). The CENP-C C-terminus has multiple functions, including M18BP1 recruitment (Dambacher et al., 2012), MEIKIN recruitment (Kim et al., 2015), and dimerization (Sugimoto et al., 1997).

(B) Signatures of positive selection are found in the kinetochore interaction domain and histone fold domain of CENP-T. CDK1-dependent phosphorylation at Thr195 and Ser201 in human CENP-T (substituted with Leu and Thr, respectively, in mice) regulates MIS12 recruitment (Rago et al., 2015; Veld et al., 2016). Signatures of positive selection are detected around these regulatory residues for MIS12 recruitment. Some DNA interacting residues within the histone fold domain are shown (Nishino et al., 2012).

(C) Signatures of positive selection are found in the domain of KNL1 that recruits BUB1 via repeated MELT motifs (Krenn et al., 2013). One MELT motif is shown as an example.

(D) Signatures of positive selection are found in domains of INCENP that interact with Borealin/Survivin, with heterochromatin, and with Aurora B kinase. Heterochromatin recruits INCENP (Abe et al., 2016; Ainsztein et al., 1998; Kang et al., 2011), and Borealin mediates the interaction with SGO1/2 (Tsukahara et al., 2010). Survivin binds cohesin and pH3T3 at pericentromeres (Kelly et al., 2010; Wang et al., 2010; Yamagishi et al., 2010), providing another mechanism to localize the CPC. A PxVxI motif, which interacts with the HP1 chromoshadow domain, is present in some Murinae species and lost in others, shown with *Mus musculus* (Mm) and *Rattus norvegicus* (Rn) as examples. Other species from the phylogenetic tree in Figure 4B: *Mus spretus* (Ms), *Mus caroli* (Mc), *Mus pahari* (Mp), *Hylomyscus alleni* (Ha), *Praomys delectorum* (Pd), *Mastomys natalensis* (Mn), *Grammomys dolichurus* (Gd), *Rhabdomys dilectus* (Rd), and *Rhynchomys soricoides* (Rs).

**A**

**Parallel Pathway Model**

<b>Drive</b>	(1) Selfish centromere DNA evolves to recruit more effectors through the kinetochore pathway (4) Selfish centromere DNA maintains CENP-B boxes because CENP-B recruits effectors
<b>Suppression</b>	(2) CENP-B equalizes centromeres through the heterochromatin pathway (3) Proteins in both pathways evolve to modulate effector recruitment

**B**

CENP-B initiates heterochromatin propagation to suppress functional differences between centromeres



Invasion of heterochromatin into CENP-A chromatin compromises segregation fidelity



CENP-B recruits CENP-C to maintain CENP-A chromatin



**Figure 6: Summary of parallel pathway model and dual functions of CENP-B in heterochromatin and CENP-A chromatin.**

(A) Selfish centromere DNA recruits more effector proteins through the kinetochore pathway to drive (1). CENP-B equalizes centromeres through the symmetric heterochromatin pathway (2), but the asymmetric kinetochore pathway is dominant in our hybrid model system. Proteins in both pathways evolve to functionally equalize genetically different centromeres by modulating effector recruitment (3). Selfish centromere DNA can evolve again to recruit more effector proteins. However, CENP-B boxes will be maintained because CENP-B recruits effector proteins (4).

(B) CENP-B initiates heterochromatin formation to equalize centromeres (top). Despite the difference in CENP-B binding sites, larger and smaller centromeres have similar amounts of H3K9me3 (Figure 1D), indicating that heterochromatin formation is insensitive to CENP-B abundance, likely due to self-propagation of heterochromatin. Invasion of heterochromatin into CENP-A compromises centromere function (middle). To prevent this disruption, we propose that CENP-B has acquired an additional function in CENP-A chromatin (bottom): CENP-B recruits CENP-C but does not contribute to CENP-C asymmetry between larger and smaller centromeres (Figure 3C), suggesting that only CENP-B within CENP-A

chromatin recruits CENP-C. Thus, CENP-B functions in heterochromatin and CENP-A chromatin are insensitive to repeat expansion.

Author Manuscript

Author Manuscript

Author Manuscript

Author Manuscript